Store-Operated Response in CA1 Pyramidal Neurons Exhibits Features of Homeostatic Synaptic Plasticity

Wissam Nassrallah

A thesis submitted to the
Faculty of Graduate and Postdoctoral Studies
in partial fulfillment of the requirements for the
MSc degree in Neuroscience

Cellular and Molecular Medicine
Faculty of Medicine
University of Ottawa

Acknowledgements

I would like to thank Dr. Jean-Claude Béïque for his continuous support of my work. In addition to granting me his unwavering attention throughout my Master's project, he has been an invaluable support in all my endeavours. My time in Dr. Béïque's laboratory not only strengthened my passion for neuroscience, but also sparked and caused to bloom within me a genuine interest and stronger appreciation for scientific research as a whole.

Also, I would like to take this opportunity to thank, Cary Soares, Kevin Lee, and Adrian Wong. They helped me greatly in understanding the intricacies of this project and the many mechanisms at play during plasticity in the brain.

I would also like to thank all other members of Drs. Béïque and Bergeron's labs for their help an support, and for making the days enjoyable, exciting, and unexpected.

Finally, I would like to thank my thesis advisory committee members, Drs. Maler and Tuana, for all the helpful advice and insight they have given me throughout the completion of this project.

Abstract

Homeostatic synaptic plasticity (HSP) regulates synaptic strength in response to changing neuronal firing patterns. This form of plasticity is defined by neurons' ability to sense and over time integrate their level of firing activity, and to actively maintain it within a defined range. For instance, a compensatory increase in synaptic strength occurs when neuronal activity is chronically attenuated. However, the underpinning cellular mechanisms of this fundamental neural process remain poorly understood. We previously found that during activity deprivation, HSP leads to an increase in α-amino-3-hydroxy-5-methyl-4-isoxazolepropionic (AMPA) receptor function as well as a shift in subunit composition from **Ca^{2+}-impermeable** GluA2-containing AMPA receptors to **Ca^{2+}-permeable** GluA2-lacking AMPA receptors not only at synapses, but also at extrasynaptic sites. Neurons therefore appear to be actively enhancing Ca^{2+} entry, possibly as a compensatory mechanism in response to a prolonged Ca^{2+} deficit. To test whether the homeostatic response may, at least in part, be mediated by internal Ca^{2+} stores, we depleted endoplasmic reticulum (ER) Ca^{2+} stores by using the Sarco/endoplasmic reticulum Ca^{2+} ATPases (SERCA) pump blocker cyclopiazonic acid (CPA) for a prolonged period. Interestingly, we have found that prolonged Ca^{2+}-store depletion leads not only to an increase in synaptic strength *per se*, but also a cell-wide increase in synaptic **Ca^{2+}-permeable** GluA2-lacking AMPARs. This increase in Ca^{2+} influx following periods of inactivity is conceptually highly reminiscent of a store-operated response, whereby cells re-establish their calcium levels following Ca^{2+} store depletion using cell surface Ca^{2+} channels. Our results suggest that neurons use synaptic receptors as means to regulate store Ca^{2+} levels, thus significantly expanding our understanding of the repertoire used by neurons to modulate cellular excitability.

Résumé

La plasticité synaptique homéostatique (HSP) régule la force synaptique en réponse aux modèles changeants de décharge neuronale. Ce type de plasticité est déterminé par la capacité des neurones à détecter et à intégrer avec le temps leur niveau d'excitabilité, et à le maintenir dans un intervalle défini. Par exemple, un accroissement compensatoire de la force synaptique a lieu lorsque l'activité neuronale est chroniquement atténuée. Cependant, les mécanismes cellulaires sous-jacents de ce processus neuronal fondamental restent mal compris. Nous avons précédemment constaté que, durant une période de privation d'activité, HSP mène à une augmentation dans la fonction du récepteur α-amino-3-hydroxy-5-methyl-4-isoxazolepropionic (AMPA) ainsi qu'à un changement dans la composition sous-unitaire du récepteur, passant de récepteurs AMPA **imperméables au Ca^{2+}** contenant GluA2, au récepteurs AMPA **perméables au Ca^{2+}** dépourvus de GluA2, non seulement aux synapses, mais aussi aux sites extrasynaptiques. Les neurones semblent donc activement améliorer l'entrée des ions Ca^{2+}, ce qui pourrait être un mécanisme compensatoire, en réponse à un manque prolongé de Ca^{2+}. Pour examiner si la réponse homéostatique pourrait, du moins en partie, être influencée par les réserves internes de Ca^{2+}, nous avons réduit les réserves de Ca^{2+} dans le réticulum endoplasmique en utilisant l'acide cyclopiazonique (CPA) pour bloquer les pompes Sarco/endoplasmic reticulum Ca^{2+} ATPases (SERCA) pour une longue période de temps. D'ailleurs, nous avons trouvé que la réduction prolongée des réserves de Ca^{2+} mène non seulement à une croissance dans la force synaptique en soi mais aussi à une croissance de récepteurs AMPA synaptiques **perméables au Ca^{2+}** dépourvus de GluA2. Une telle croissance, advenue après des périodes d'inactivité, rappelle fortement une réponse contrôlée par les réserves, selon laquelle les cellules rétablissent leurs niveaux de Ca^{2+}, à

la suite de la réduction de ces réserves, en utilisant les canaux Ca^{2+} situés dans la membrane plasmique. Nos résultats suggèrent que les neurones utilisent des récepteurs synaptiques comme un moyen pour réguler les niveaux des réserves de Ca^{2+}, élargissant ainsi considérablement notre compréhension du répertoire utilisé par les neurones pour moduler l'excitabilité cellulaire.

Table of Contents

List of Figures

List of Abbreviations

AHP	-	Afterhyperpolarisation
AMPA	-	α-amino-3-hydroxy-5-methyl-4-isoxazolepropionic
AMPAR	-	α-amino-3-hydroxy-5-methyl-4-isoxazolepropionic receptors
CaMKII	-	Calmodulin-dependent protein kinase II
CaMKIV	-	Calmodulin-dependent protein kinase IV
CCE	-	Capacitative Ca^{2+} entry
CICR	-	Calcium-Induced Calcium Release
CNS	-	Central Nervous System
CPA	-	Cyclopiazonic acid
CRAC	-	Ca^{2+} release-activated Ca^{2+} channels
D-APV	-	D-2-amino-5-phosphonovalerate
EPSC	-	Excitatory post-synaptic current
ER	-	Endoplasmic Reticulum
GABA	-	gamma amino butyric acid
HSP	-	Homeostatic Synaptic Plasticity
LTD	-	Long-Term Depression
LTP	-	Long-Term Potentiation
mEPSC	-	Miniature excitatory post-synaptic current
NMDA	-	N-methyl-D-aspartate

NMDAR	-	N-methyl-D-aspartate receptor
SA	-	Spine apparatus
SD	-	Synaptopodin
SERCA	-	Sarco/endoplasmic reticulum Ca^{2+} ATPases
SOC	-	Store-operated Ca^{2+} channels
STDP	-	Spike Timing Dependent Plasticity
STIM-1	-	Stromal interaction molecule 1
Syn-YFP	-	Synapin-YFP
TTX	-	Tetrodotoxin
VGCC	-	Voltage-gated calcium channels

1. Introduction

1.1 Glutamate Synapses

The brain consists of billions of neurons with distinct functions and structures. The way these neurons are connected with each other make up the powerful computer that reacts to our environment in various ways. In fact, each neuron has thousands of these connections known as synapses (Spruston, 2008). The vast majority of cortical synapses can generally be categorized as inhibitory, mediated by gamma amino butyric acid (GABA), or excitatory, mediated by glutamate (Kandel *et al.*, 2000). Here, I will focus on the excitatory synapses. Glutamate receptors can be ionotropic (pore-forming) or metabotropic (G-protein coupled receptors) (Traynelis *et al.*, 2010). At central neurons, such CA1 pyramidal neurons in the hippocampus, the main ionotropic glutamate receptors are the α-amino-3-hydroxy-5-methyl-4-isoxazolepropionic (AMPA) and N-methyl-D-aspartate (NMDA) subtypes. AMPA receptors have the "reputation" of being the 'workhorse' of the synapse because they provide the major excitatory driving force at resting membrane potentials. While both AMPA and NMDA receptors require the glutamate to gate, the latter also requires depolarization of the neuron to expel the magnesium (Mg^{2+}) block from its pore (Mayer *et al.*, 1984; Nowak *et al.*, 1984; Johnson and Ascher, 1987; Kleckner and Dingledine, 1988; Lerma *et al*., 1990). Therefore, NMDA receptors are not only ligand dependent but also voltage dependent hence a coincident detector. Both receptors are located at synaptic and extrasynaptic sites. Furthermore, the expression of these receptors are constantly regulated at the plasma membrane (Traynelis *et al.*, 2010).

1.2 Glutamate Receptors

1.2.1 Ionotropic Glutamate Receptors: NMDA Receptors

The role of NMDA receptors in excitatory neurotransmission regulation is vital in the CNS. NMDA receptors are cationic channels permeable to Na^+, K^+, and Ca^{2+} (Perez-Otano & Ehlers, 2005). The Ca^{2+} influx through NMDA receptors is critical in many of the NMDA receptors physiological and pathophysiological processes (Cull-Candy & Leszkiewicz, 2004). Genetic deletion of the GluN1 subunit causes death in neonatal stages. Furthermore, GluN1 constitutes a necessary subunit of all NMDA receptors (Forrest *et al*., 1994). The C-terminus region of GluN1 regulates NMDA receptor trafficking and binding to proteins, including calmodulin, CaMKII, yotiao, alpha-actinin, tubulin, neurofilaments, and downstream regulatory element antagonist modulator (DREAM; Cull-Candy & Leszkiewicz, 2004; Horak & Wenthold, 2009).

The combination of two GluN1 subunits with two GluN2 subunits (GluN2A – GluN2D) or a combination of GluN2 and GluN3 subunits (GluN3A – GluN3B) is essential for the formation of functional NMDA receptors (Monyer *et al*., 1992; Schorge and Colquhoun, 2003; Ulbrich and Isacoff, 2007, 2008; Traynelis *et al*., 2010). NMDA receptors are also coincident detectors. They require simultaneous binding of both glutamate and glycine for activation, and also require depolarisation to expel the magnesium (Mg^{2+}) block from its pore (Johnson and Ascher, 1987; Kleckner and Dingledine, 1988; Lerma *et al*., 1990). Therefore, NMDA receptors are not only ligand dependent but also voltage dependent hence a coincident detector. The glycine binding site resides on the GluN1 and GluN3 subunits (Furukawa and Gouaux, 2003; Furukawa *et al*., 2005;

Yao *et al*., 2008), while the glutamate binding site is located on the GluN2 subunits (Furukawa *et al*., 2005). NMDA receptors are not functional without the GluN2 subunit in mammalian cells.

1.2.2 Ionotropic Glutamate Receptors: AMPA Receptors

AMPA receptors are the driving force of excitatory synaptic transmission in the CNS. They are ionotropic glutamate receptors which are transmembrane proteins comprised of four large subunits (more than 900 residues each), which are localized at neuronal and non-neuronal cells. The four subunits constitute a central ion channel pore. Ionotropic glutamate receptor subunits contain four domains: an extracellular amino-terminal domain, an extracellular ligand-binding domain, a transmembrane domain, and an intracellular carboxyl-terminal domain.

The majority of fast excitatory synaptic neurotransmission in the central nervous system (CNS) is mediated by glutamate activation of AMPA receptors (Dingledine *et al*., 1999). AMPA receptors are comprised of a combination of four subunits (GluA1 – GluA4) (Traynelis *et al*., 2010). In general, native AMPA receptors are thought to be heterotetramers. For instance, in mature rats, the most common subunit configurations of AMPA receptors in hippocampal pyramidal cells are GluA1/GluA2 and GluA2/GluA3 (Dingledine *et al*., 1999; Traynelis *et al*., 2010). The GluA2 subunit of AMPA receptors governs their permeability to calcium ions (Ca^{2+}). The presence of a GluA2 subunit renders the channel impermeable to Ca^{2+} due to the posttranslational mRNA editing of a glutamine (Q) to an arginine (R) residue (Seeburg & Hartner, 2003). The majority of GluA2 subunits in the CNS are found in the GluA2(R) form, making most AMPA receptors permeable only to sodium ions (Na^{+}) and potassium ions (K^{+}), and not permeable

to Ca^{2+} (Dingledine *et al*., 1999). On the contrary, AMPA receptors containing an unedited 'Q-form' of GluA2 or lacking the GluA2 subunit are permeable to Ca^{2+} (Sommer *et al*., 1991).

It has been shown that an imbalance between Ca^{2+}-impermeable AMPA and Ca^{2+}-permeable AMPA receptors have been related to the development of epilepsy (Tanaka *et al*., 2000). In fact, seizure susceptibility in adult rat brains is increased by the presence of the Ca^{2+}-permeable AMPA receptors, and that these types of receptors play a role in circuit hyper-excitability (Krestel *et al*., 2004). Furthermore, susceptibility to hypoxia-induced seizures occurs in the brain during developmental stages when there is an increased expression of Ca^{2+}-permeable AMPA receptors. Consequently, perinatal hypoxia-induced seizures increase the expression of Ca^{2+}-permeable AMPA receptors and the capacity for an AMPA receptor–mediated epileptogenesis (Sanchez *et al*., 2001). Therefore, elucidating the effects of plasticity on the expression of Ca^{2+}-permeable AMPA receptors and studying the mechanisms by which Ca^{2+}-permeable AMPA receptors are regulated are vital to understand the causes of epileptogenesis.

1.3 Hebbian Plasticity

The regulation of glutamate receptors is an integral mechanism in synaptic plasticity which is the neurons ability to modify its synaptic properties (glutamate receptors included) in response to various stimuli (Malenka and Bear, 2004). With this in mind, changes in information coding and memory in the brain are partly underlied by the modulation of signaling between neurons at synapses. The modulation of the strength of synapses may be at the basis of learning. This process is largely believed to be governed by Hebbian forms of synaptic plasticity, such as Long-Term Potentiation (LTP) and Long-Term Depression (LTD) (**Figure 1 A and B**). LTP and LTD are

mediated by the dynamic regulation of postsynaptic glutamate receptors of the AMPA and NMDA subtypes (**Figure 1 C**). These processes display many of the features described in a model suggested by Donald Hebb, around 60 years ago, to explain how a neuronal network is able to store information (Hebb, 1949). Consequently, substantial efforts have been devoted towards defining the cellular and molecular mechanisms of LTP and LTD, and to understand their roles in learning and memory (Malenka & Nicoll, 1999; Malinow & Malenka, 2002; Lisman & Raghavachari, 2006; Whitlock *et al*., 2006; Kerchner & Nicoll, 2008; Kessels & Malinow, 2009). Today, these activity-dependent synaptic plasticity mechanisms are well described, and are thought to underlie information storage in the brain.

LTP is a long-term enhancement of signal transmission between two neurons which can be the result of a high frequency stimulation of the presynaptic neuron (**Figure 1 A**). LTD is a long-term decrease in the efficacy of signal transmission between two neurons due to low frequency stimuli (**Figure 1 B**). Hebbian LTP and LTD occur within seconds to minutes, in response to relatively short bouts of synaptic stimulation, and they can last from hours to days (Abraham, 2003). Another method by which Hebbian Plasticity can be induced in neurons is by a phenomenon called Spike Timing Dependent Plasticity (STDP). Through this paradigm, synaptic strength can be altered by the timing of pre- and postsynaptic spikes. Essentially, LTP can be achieved if postsynaptic firing is preceded by synaptic input (originating from presynaptic spikes). Furthermore, LTD occurs when postsynaptic spikes precedes synaptic input (Markram *et al.*, 1997). STDP only operates when pre- and postsynaptic activities are within 30 milliseconds of each other (Bi & Poo, 1998; Feldman, 2000; Sjostrom *et al.*, 2001).

Generally, Hebbian Plasticity requires the influx of calcium through the opening of NMDARs (Collingridge *et al.*, 1983; Lynch *et al.*, 1983). The alteration in synaptic strength is

then expressed through up- or downregulation of postsynaptic AMPARs (Malinow & Malenka, 2002; Shepherd & Huganir, 2007). Furthermore, the calcium-dependent activation of calmodulin-dependent protein kinase II (CaMKII) is required for this process (Malinow *et al.*, 1988; Malinow *et al.*, 1989). What is certain is the importance of glutamate receptors in this mechanism. NMDARs act as the inducers of Hebbian Plasticity while changes in AMPAR function reflect the expression of this phenomenon. Though I have given a relatively thorough overview of Hebbian Plasticity, this was to contextualize Homeostatic Synaptic Plasticity, which is the focus of my thesis.

1.4 Homeostatic Synaptic Plasticity

1.4.1 Problems with Hebbian Plasticity

The implementation of only Hebbian-type LTP and LTD mechanisms in different neuronal network models proved to be problematic in network function stability (Miller and MacKay, 1994; Turrigiano & Nelson, 2004; Lazar *et al.*, 2009). These models establish a fundamental problem with an exclusive positive-feedback mechanism, such as Hebbian plasticity. In a network expressing purely Hebbian plasticity rules, synapses are driven to an excess of potentiation and depression, causing some synapses to reach a functional plateau, while others become functionally inactive (**Figure 2**). These positive-feedback processes may lead to the development of epileptogenic activity in neurons (Turrigiano & Nelson, 2004; Lazar *et al*., 2009). As Wong (2005) suggested, brain development in young children is intensive, and LTP/LTD have been associated with making children more susceptible to seizure. Nevertheless, several studies have shown that the occurrence of seizures in young children remains fairly low, taking into account the extent of

developmental changes involved in early childhood, suggesting the possibility of negative-feedback mechanisms which would lead to the stabilization of neural networks during development (Turrigiano and Nelson, 2004; Davis, 2006) and during mature brain function (Yeung *et al*., 2004; Toyoizumi *et al*., 2005; Houweling *et al*., 2005; Thivierge & Cisek, 2008; Turrigiano, 2008; Lazar *et al*., 2009; Turrigiano, 2012).

1.4.2 Solution to the Instability Problem

Homeostatic plasticity mechanisms that maintain the firing activity of neurons within a determined range have been identified. As such, neurons can keep their spiking activity within an ideal range, and therefore play the role of stable carriers of information in brain activity (**Figure 3**). Numerous determinants of cellular excitability, such as intrinsic excitability (Grubb and Burrone, 2010; Turrigiano, 2011) and synaptic strength (O'Brien *et al*., 1998; Turrigiano *et al*., 1998; Turrigiano & Nelson, 2004; Turrigiano, 2012) are regulated by neurons to reach homeostasis, which is to keep the firing rate of a neuron within an optimal range. More precisely, the finding of homeostatic synaptic plasticity (HSP) has sparked substantial attention since it offers a possible way to resolve the aforementioned instability problem of Hebbian networks. Having characteristics similar to denervation supersensitivity at the neuromuscular junction (Cannon, 1949), HSP is described as a bidirectional regulation of synaptic transmission in response to prolonged modifications in network activity (O'Brien *et al*., 1998; Turrigiano *et al*., 1998; Turrigiano, 2008). It has been suggested, however, that STDP alone may be enough to solve the instability problem previously described (Abbott & Nelson, 2000). Nevertheless, HSP offers another dimension of complexity in the control of synaptic function.

One of the determinants of cellular excitability in the maintenance of homeostasis is the strength of excitatory glutamatergic synapses. On one hand, the prolonged reduction of a neuron's firing activity leads to the reinforcement of its excitatory synapses. On the other hand, the prolonged enhancement of its firing activity results in the weakening of its excitatory synapses (**Figure 4**). These processes are known as HSP, and are gradually becoming accepted as essential neuronal mechanisms for stability of neural networks.

HSP is often studied by pharmacologically blocking neuronal network activity with tetrodotoxin (TTX) – a voltage-gated sodium channel blocker – for several days (Sutton *et al.*, 2006; Soden & Chen, 2010; Groth *et al.*, 2011; Lindskog *et al*., 2011). Neurons respond to this prolonged suppression of activity by a cell-wide up-regulation of synaptic AMPA receptors to enhance cellular excitability. This cell-wide synaptic regulation is bidirectional, that is, neurons also tune down excitability by down-regulating synaptic AMPA receptors in response to prolonged elevations in activity. This response is suggested to be triggered by alterations in calcium signalling due to changes in voltage-gated calcium channel (VGCC) activation frequency. This was proposed to lead to changes in regulation by CaMKIV of gene expression (Ibata *et al.*, 2008; Goold & Nicoll, 2010). One interesting aspect of this global form of HSP is its multiplicative nature (O'Brien *et al*., 1998; Turrigiano *et al*., 1998; Lee *et al*., 2013). Multiplicativity refers to the observation that when neurons undergo HSP, the distribution of miniature excitatory postsynaptic current (mEPSC) amplitudes is changed by a single common factor. The most important implication of such multiplicativity is that each synapse of a neuron must "scale" up in a manner proportional to its original synaptic strength. As a result, neurons can tune cellular excitability without disrupting the relative strengths between synapses, thus preserving the catalogue of synaptic engrams previously encoded, perhaps, by Hebbian plasticity mechanisms.

Various forms of cell-wide and input specific HSP have been identified. There have been several insights utilising *in vivo* paradigms to study this phenomenon. For example, with visual plasticity, raising animals in the dark, intraocular TTX injections, or binocular enucleation all led to an increase in AMPAR-mediated mEPSCs in V1 layer 2/3 pyramidal neurons (Desai *et al.*, 2002; Goel *et al.*, 2006; Goel & Lee, 2007; Gao *et al.*, 2010) (reviewed in Whitt *et al.*, 2014). Similarly, an increase in excitatory synaptic strength was observed in L2/3 of A1 following sensory neuronal hearing loss, a method that removes evoked and spontaneous activity from the sensory organ (Kotak *et al.*, 2005). Furthermore, abolishing all tactile whisker driven activity in 4-week old rats by unilateral infraorbital nerve resection led to the potentiation of thalamocortical inputs to the rodent barrel cortex (Yu *et al.*, 2012). These results suggest the importance of HSP in our ability to adapt to radical changes in our environment. Beyond cell-wide forms of HSP, input specific HSP has helped shape our understanding of the purpose of HSP. For instance, the existence of input specific HSP was verified *in vivo*. Neurons of the optic tectum in Xenopus tadpoles, which receive inputs from visual and mechanosensory pathways, provided an excellent avenue to study the synapse specificity of HSP. It was observed that only synapses of the visual pathway were potentiated after dark-rearing of tadpoles, whereas overstimulation of the mechanosensory pathway by constant vibration led to only mechanosensory synapses being depressed (Deeg & Aizenman, 2011). Furthermore, it has been shown that prolonged activity deprivation by TTX leads to synapse-specific effects for CA3 pyramidal neurons. Whereas feed-forward synapses potentiate after this form of HSP, recurrent CA3-CA3 synapses were depressed, thus showing an added level of complexity whereby glutamatergic synapses react differently to the same stimulus (in this case, TTX). In this manner, the weakening of these reverberant synapses was said to stabilise the network by reducing epileptic activity (Kim & Tsien, 2008).

One group demonstrated the presence of input-specific HSP in an ingenious way. Béïque *et al.* overexpressed Kir2.1 (to suppress the synaptic activity of a small subset of synapses) and Synapin-YFP (Syn-YFP) (to visualize synaptic terminals) in neurons. Using two-photon glutamate uncaging, synapses receiving input from these Kir2.1 overexpressed neurons showed an increases in post-synaptic AMPAR currents when compared to control spines (Beique *et al.*, 2011). Furthermore, this increase in AMPARs was accompanied by a subunit compositional change from **Ca^{2+}-impermeable** GluA2-containing AMPA receptors to **Ca^{2+}-permeable** GluA2-lacking AMPA receptors. This process was shown to be dependent on the immediate early gene Arc. Altogether, individual synapses are able to regulate themselves independently of the firing rate of the neuron as a whole. This finding led to a paradigm shift in our understanding of HSP in that despite the neurons firing rate being largely unaffected, the neuron is able to measure synaptic input of individual spines and regulate their strengths accordingly. It is likely that cell-wide HSP and synapse-specific HSP both coordinate to maintain synaptic function within a range that is optimal for neural computation.

Although the phenomenon of HSP is now relatively well established, several molecular details of HSP expression at synapses remain poorly understood. Recently, we investigated AMPAR subunit composition through biophysical and pharmacological methods after 3-4 days TTX treatment (Soares *et al.*, 2013). It is well established that AMPARs containing the GluA2 subunit exhibit linear current-voltage (I-V) relationships, while GluA2-lacking AMPARs exhibit inward rectification at positive potentials due to channel blockade by intracellular polyamines (Bowie and Mayer, 1995). We thus used this biophysical signature to probe the GluA2-content of synaptic AMPARs. We calculated the rectification indices of I-V curves constructed from pharmacologically-isolated AMPAR-mediated evoked excitatory postsynaptic currents (eEPSCs)

at Schaffer-collateral (SC) synapses in the presence of (100 μM) intracellular spermine (Beique *et al*., 2011). Spermine was used to provide the polyamine needed to induce the characteristic inwardly rectifying polyamine block of GluA2-lacking AMPARs. AMPAR-mediated eEPSCs from control neurons displayed linear I-V relationship, consistent with the presence of predominantly GluA2-containing AMPARs at these synapses (Lu *et al*., 2009). In contrast, we detected a strong voltage-dependent block of AMPAR-eEPSCs in TTX treated neurons, suggesting the presence of synaptic GluA2-lacking AMPARs. This shift in AMPAR subunit composition grants a Ca^{2+} permeability to these new GluA2-lacking AMPARs previously absent from GluA2-containing AMPARs. Furthermore, this shift in AMPA receptor subunit composition is a cell-wide phenomenon happening at spines, dendritic shafts, and the soma (Soares *et al.*, 2013) (**Figure 5)**. In other words, the neuron is, for some reason, actively introducing a new source of calcium (**Figure 6**).

1.5 Store-Operated Responses in the Endoplasmic Reticulum (ER)

We previously found that HSP leads to the insertion of Ca^{2+} permeable GluA2-lacking AMPARs not only at synaspes, but at extrasynaptic sites as well. Although this switch in subunit composition of AMPARs bears strong functional implications for synapse function, it also increases calcium influx in neurons in response to ongoing synaptic activity. Extrasynaptic sites also contribute to this increase in calcium influx due to glutamate spill over from the synapse. Such an increase in calcium influx following periods of inactivity is highly reminiscent of a store-operated response, whereby cells restore their intracellular calcium stores following depletion.

This raises the possibility that the homeostatic response may, at least in part, be a store-operated response.

Briefly, this response occurs during Ca^{2+} emptying of ER stores (through Ryanodine receptors, IP3 receptors, or Ca^{2+} leak channels), where mechanisms with the purpose of refilling these stores are triggered (Alonso *et al.,* 1991). A transverse ER membrane Ca^{2+} sensor – Stromal interaction molecule (STIM1) – senses the depletion of Ca^{2+} with its N-terminal tail (Roos *et al.,* 2005). STIM1 then aggregates and migrates to the ER-plasma membrane junction and activates Ca^{2+} channels at the plasma membrane (Luik *et al.,* 2006). Channels that are activated by the depletion of $[Ca^{2+}]_{ER}$ are referred to as store-operated Ca^{2+} channels (SOC) or Ca^{2+} release-activated Ca^{2+} channels (CRAC). One example of a CRAC channel is the plasma membrane pore-forming protein Orai1 (Cahalan *et al.,* 2007). The main purpose of these channels is to refill the ER of its Ca^{2+} store following depletion. While the ER and the plasma membrane are in close proximity (around 10 nm), there is actually no physical contact between the two. However, a tight coupling between the influx of Ca^{2+} through CRAC channels and the influx of Ca^{2+} into the ER through sarco/endoplasmic reticulum Ca^{2+} ATPases (SERCA) has been observed (Alonso *et al.,* 2012). These mechanisms are referred to as capacitative Ca^{2+} entry (CCE) or store-operated responses (**Figure 7**).

Importantly, the phenomenon of AMPARs refilling calcium stores after prolonged calcium depletion would be of significant impact in that it would show that neurons use synaptic receptors as means to regulate store calcium homeostasis, significantly expanding our understanding of the cellular machinery of store operated responses in central neurons.

2. Objectives and Hypotheses

In order to explore the possibility that synaptic channels are used to refill calcium ER after depletion, we reasoned that prolonged ER calcium store depletion would cause a subunit switch from calcium impermeable GluA2-containing AMPARs to calcium permeable GluA2-lacking AMPARs. Confirming the link between homeostatic and store-operated responses would bring a significant paradigm shift in our understanding of this fundamental cellular mechanism.

To determine whether the regulation of a population of glutamate receptor subunits is part of the store-operated response in central neurons, we treated hippocampal organotypic slices with cyclopiazonic acid (CPA) for 2 days. CPA acts as a pore-blocker of SERCA pumps, thus preventing refilling of ER Ca^{2+} stores and the eventual depletion of these stores (Moncoq *et al*., 2007). We then assessed whether Ca^{2+} emptying of ER stores causes the potentiation of AMPARs and/or the insertion of GluA2-lacking AMPARs at the plasma membrane (synaptically and/or extrasynaptically) of CA1 hippocampal neurons.

It is well established that AMPARs containing the GluA2 subunit exhibit linear current-voltage (I-V) relationships, while GluA2-lacking AMPARs exhibit inward rectification at positive potentials due to channel blockade by intracellular polyamines (Bowie and Mayer, 1995). We used this biophysical property to probe the GluA2-content of synaptic AMPARs.

Objective 1: To determine whether the regulation of a population of glutamate receptor subunits is part of the store-operated response in central neurons (**Figure 9 A**).

Hypothesis: Depletion of ER Ca^{2+} stores will cause a shift from calcium impermeable GluA2-containing to calcium permeable GluA2 lacking AMPARs.

Objective 2: To determine whether homeostatic synaptic plasticity is a store operated response (**Figure 9 B**).

Hypothesis: HSP induced by TTX and the store-operated response act through the same mechanism.

3. Materials and Methods

To tackle both objectives, we used rat hippocampal organotypic tissue cultures. These cultures allow for prolonged pharmacological treatments while maintaining the neuronal structure and synapses of the brain tissue in question which in this case is the hippocampus.

3.1 Organotypic Slice Culture

Organotypic slice cultures are prepared using a modified method of the original technique reported by Stoppini *et al*. 1991. Sprague-Dawley rats (Charles River Laboratories; 6-8 days old) are anaesthetized by isofluorane (Baxter Corporation, Canada) inhalation and decapitated according to methods approved by the University of Ottawa Animal Care Committee. Individual hippocampi are removed in ice-cold cutting solution containing the following (in mM): 119 choline chloride, 2.5 KCl, 4.3 MgSO4, 1.0 CaCl2, 1.0 NaH2PO4–H2O, 1.3 Na-ascorbate, 11 glucose, 1 kynurenic acid, 26.2 NaHCO3, saturated with 95% O2 and 5% CO2, pH 7.3 (295–310 mOsm/L), and coronal hippocampal slices (400 μm) are obtained using an MX-TS Tissue Slicer (Siskyou). Individual hippocampal slices are transferred to membrane inserts (Millipore, #PICM03050) and maintained in six-well plates at 34°C in 95% O_2 and 5% CO_2 containing

Neurobasal-A-based culture media. Slice culture media is exchanged at 1 day in vitro (DIV) and then every 2-3 days thereafter. After 6-8 DIV, slices are divided into treatment and control groups; 30 µM cyclopiazonic acid (CPA, Abcam Biochemicals, #ab120300) is added to the treatment group. The treatment lasts for 48 hours.

Objective 1:

3.2 Whole-Cell Electrophysiology

Whole-cell recordings were performed on CA1 pyramidal neurons in treated and control slices after 2 days of CPA-treatment. Slices were removed from culture inserts, placed in a recording chamber, and CA1 pyramidal cells were visualized under differential-interference contrast (DIC) using a Zeiss Axio Examiner D1 upright microscope (40x/0.75NA objective). All experiments were performed at room temperature (23-25°C) in artificial cerebrospinal fluid (ACSF) containing the following (in mM): 119 NaCl, 2.5 KCl, 1.3 MgSO4, 2.5 CaCl2, 1.0 NaH2PO4, 11 glucose, and 26.2 NaHCO3 saturated with 95% O2 and 5% CO2, pH 7.3 (295–310 mOsm/L). Additional drugs were added to the ACSF as follows (in µM): 1 TTX (Tocris Bioscience), 150 picrotoxin (Tocris Bioscience), and 50 D-APV (abcam Biochemicals). Picrotoxin and D-APV were included to block GABA and NMDA receptors respectively in order to study AMPARs. Cells were recorded using an Axon Multiclamp 700B amplifier, sampled at 10 kHz, digitized with an Axon Digidata 1440A digitizer and Bessel filtered at 2 kHz. Borosilicate glass recording electrodes (World Precision Instruments, Florida or Sutter, California) were pulled using a Narashige PC-10 vertical puller (Narishige, Japan), and had resistances ranging from 3.5-5 MΩ. For AMPAR I-V curves, 0.1 mM spermine (Tocris) was included in the internal solution, and the

recordings were done in voltage-clamp mode. For all voltage-clamp recordings, access resistance was continuously monitored during the experiment by delivering a 5 mV hyperpolarizing step at the beginning of each trace. All recordings were analyzed using Clampfit 10.2 (Molecular Devices) and Origin 8 analysis software (OriginLab).

3.3 Two-Photon (2P) Imaging and Uncaging

Simultaneous two-photon imaging and glutamate uncaging was performed using two ultrafast Ti:Sapphire on an Olympus MPE-1000 system (BX61WI upright microscope; 40x/0.8NA or 60x/1.0NA objective; Olympus, Melville, NY). We filled the cell with 0.03 mM Alexa Fluor 594 hydrazide (Na-salt; Invitrogen) using the recording pipet allowing us to image the cell with a 2P laser set at 810 nm. In this manner, we visualized the morphology of the cell, including its spines and dendritic arborisation. While imaging, the cell was in a bath of ACSF containing 2.5 mM MNI-Glutamate trifluoroacetate (Femtonics), 1 μM TTX (Tocris Bioscience), 150 μM picrotoxin (Tocris Bioscience), and 50 μM D-APV (Abcam Biochemicals). MNI-Glutamate cannot interact with AMPARs unless uncaged with a 2P laser set at 720 nm. Controlling the power of the laser allows one to control the amount of glutamate uncaged, and thus enables the recording of a single synapse, estimated at the tip of a spine visualised with the 810 nm laser. I-V curves of AMPARs from synaptic, extrasynaptic, and soma loci were studied in this fashion.

Objective 2:

3.4 Biolistic Transfection

The cells were transfected biolistically using the same procedure as described by Soares *et al*., 2014. Neurons were co-transfected with mCherry (Takara Clontech, Mountain View, CA) to visualize the morphology of the neuron and pHluorin-GluA2 ΔC49 (Rathje *et al*., 2013) to visualize the endoplasmic reticulum (ER). We then used the spine enrichment index to measure the amount of ER in spines.

G_{sp} = Value of the intensity in the green channel at a spine

R_{sp} = Value of the intensity in the red channel at a spine

G_{den} = Value of the intensity in the green channel at a dendritic shaft

R_{den} = Value of the intensity in the red channel at a dendritic shaft

Spine Enrichment Index

$$SEI = \frac{\text{Peak } (G_{sp}/R_{sp})}{\text{Peak } (G_{den}/R_{den})}$$

3.5 Slow AHP

We also looked at the time course of slow AHP as a proxy to assess relative calcium ER levels between various conditions. We incubated organotypic hippocampal slices in CPA (30 μM) for 3 hours, recorded the AHP of CA1 pyramidal neurons in the presence of CPA, and compared the slow AHP amplitude with that of an untreated neuron (control). The slow AHP was generated in voltage-clamp mode by holding the cell at -50 mV, depolarising the cell to 20 mV for 500 ms, and polarising the cell back to -50 mV. The depolarisation to 20 mV opens calcium channels, leading to the generation of calcium-mediated potassium currents underlying the AHP.

4. Results

4.1 AMPARs-mediated mEPSCs of CPA-treated CA1 pyramidal cells

One defining feature of TTX-induced HSP is an increase in AMPAR-mediated mEPSCs. One immediate prediction of our hypothesis is that depleting ER Ca^{2+} stores would also lead to an increase in AMPAR expression. To determine whether AMPARs are upregulated after prolonged calcium store depletion, we recorded AMPARs mEPSCs and analysed their amplitudes after incubating the organotypic hippocampal slices in CPA (30 μM) for 24 or 48 hours. Recordings were done in the presence of TTX (1 μM) and picrotoxin (150 μM). For the 24 hour CPA treatment, we did not observe a difference in the average mEPSC amplitude between control and CPA treatment ($p = 0.115$; unpaired Student's t test; n = 14 for control; n = 14 for CPA) (**Figure 10 B**). However, when all the mEPSC events are plotted in a cumulative distribution curve, we observed a significant increase in the amplitudes of the CPA-treated cells compared to the control condition (p-value < 0.001; two-sample K-S test) (**Figure 10 B**). Thus, a 24 hour treatment seems to show a significant but small change in AMPAR mEPSCs. In order to widen the gap of mEPSC amplitudes between control and prolonged calcium depleted cells, we increased the time of the CPA treatment from 24 to 48 hours. For the 48 hour CPA treatment, we observed an increase in the average mEPSC amplitude in CPA treated cells compared to the control condition ($p < 0.5$; unpaired Student's t test; n = 9 for control; n = 10 for CPA) as well as a difference in the cumulative distribution of the mEPSCs (p-value < 0.001; ks test) (**Figure 11 B**). Thus, the 48 hour CPA treatment was used for the rest of the experiments unless otherwise noted because it showed the biggest change in mEPSC amplitude.

We also analysed AMPAR mEPSC frequency to observe whether prolonged calcium depletion led to any changes in spontaneous vesicular release probability or number of synapses. The 24 hour and 48 hour CPA treatment revealed no difference in the average frequency of events between control and CPA treatment (24 hour CPA treatment, p-value = 0.189, unpaired Student's t test, n = 14 for control, n = 14 for CPA, **Figure 10 C**; 48 hour CPA treatment, p-value = 0.286, unpaired Student's t test, **Figure 11 C**). However, when the inter-event intervals were plotted in a cumulative distribution, we observed a significant difference between the frequencies of events of mEPSCs of the two conditions (24 hour CPA treatment, p-value < 0.001, two-sample K-S test, **Figure 10 C**; 48 hour CPA treatment, p-value < 0.001, two-sample K-S test, n = 9 for control; n = 10 for CPA **Figure 11 C**). The frequency of mEPSCs was greater in CPA-treated cells than in control cells. This suggests that either spontaneous vesicular release, number of synapses, or both are increased after 48 hour calcium depletion. An increased probability of vesicular release or increased number of synapses would lead to an increase in the number of mEPSC events.

4.2 Excitability of CPA-treated CA1 pyramidal cells

The increase in mEPSC amplitude observed after 48 hour CPA treatment is highly reminiscent of that observed in TTX-induced HSP. One possible explanation for this CPA-induced effect other than prolonged ER calcium store depletion is that CPA may have an effect on neural excitability. To determine whether acute CPA treatment has an effect on the excitability of CA1 pyramidal neurons, we performed current injections in CA1 pyramidal neurons in control conditions and right after calcium store depletion. To achieve calcium store depletion, we incubated slices in 30 μM CPA for 3 hours prior to patching, and the recording was performed in

the presence of CPA. CPA was applied for 3 hours in order to be certain that ER calcium stores were depleted. We recorded action potentials generated from different current injections (ranging from -20 pA to 200 pA, incrementally by 20 pA steps) in CPA-treated and untreated slices. As shown in **Figure 12 B**, there was no difference in the firing rate between control and acute CPA treated CA1 pyramidal neurons (n = 12 for control; n = 9 for CPA). Therefore, we did not detect any drastic changes in excitability following acute CPA treatment. Consequently, the increase in AMPAR mEPSC amplitude is probably not due to decreased activity of the network, but most likely to the prolonged depletion of ER calcium stores.

4.3 Stimulation-evoked AMPAR I-V curves

TTX-induced HSP leads to an increase in calcium permeable AMPARs. We hypothesise that this increase in calcium permeability is due to decreased calcium in internal stores of the neuron. Therefore, we should observe a shift in the AMPAR population from calcium impermeable GluA2-containing to calcium permeable GluA2-lacking after prolonged ER calcium store depletion. To determine whether there is a subunit shift from GluA2-containing to GluA2-lacking AMPARs after prolonged calcium store depletion, we measured stimulation-evoked AMPAR I-V curves in the presence of spermine after 48 hour CPA treatment. Toward this end, we stimulated the Schaffer collaterals with a stimulating electrode and recorded a monosynaptic current from a CA1 pyramidal neuron at different holding potentials (-60 mV, -30 mV, 0 mV, 20 mV, and 40 mV) in the presence of D-APV (50 μM) and picrotoxin (150 μM). An Ohmic I-V relationship indicates the presence of GluA2-containing AMPARs whereas an inwardly rectifying current suggests the insertion of GluA2-lacking AMPARs (**Figure 13 A**). As shown by the rectification

index averages (**Figure 13 D**), the CPA-treated slices display significantly more rectification ($p < 0.05$; unpaired Student's t test; n = 9 for control; n = 10 for CPA) (**Figure 13 E**). This suggests the insertion of GluA2-lacking AMPARs into synapses following store depletion.

4.4 Glutamate uncaging evoked AMPAR I-V curves

In TTX-induced HSP, the change in subunit composition from GluA2-containing to GluA2-lacking AMPARs occurred not only at synaptic sites, but also at other subcellular regions. Thus, we explored the possibility that prolonged calcium store depletion also leads to the same subcellular distribution of AMPARs as TTX-induced HSP. To determine whether this subunit change happens at other subcellular regions, and not just at synaptic sites, we used two-photon uncaging of MNI-glutamate to probe for GluA2-lacking AMPARs at spine, dendritic, and somatic sites of CA1 pyramidal neurons. Two-photon uncaging of MNI-Glutamate allows us to activate glutamate receptors at defined subcellular compartments. Essentially, we filled the cell with a fluorescent dye (Alexa 594) for visualisation of morphology (**Figure 14 A**), then we generated I-V curves at each subcellular site in the presence of D-APV (50 μM) (**Figure 14 B**), and the rectification index was applied here to differentiate between a GluA2-containing and a GluA2-lacking AMPA receptor population. We observed significant differences in the rectification indices at the spine ($p < 0.01$; unpaired student's t test; n = 20 for control; n = 23 for CPA), dendrite ($p < 0.01$; unpaired student's t test; n = 14 for control; n = 15 for CPA), and soma ($p < 0.01$; unpaired student's t test; n = 23 for control soma; n = 15 for CPA) between control and CPA treatment (**Figure 14 D**). In all three subcellular regions, CPA-treated cells rectified more than control cells. This suggests that prolonged ER calcium store depletion leads to a cell-wide insertion

of GluA2-lacking AMPARs, which has also been observed after TTX-induced HSP (**Figure 14 C**).

4.5 Spine density and spine volume

As reported in section ***4.1***, prolonged ER calcium store depletion led to an increase in AMPAR mEPSC amplitude and frequency. The increase in mEPSC amplitude may indicate spine enlargement, since bigger spines are correlated with synapses having a higher content of AMPARs. Furthermore, the increase in mEPSC frequency suggests a larger number of synapses. Therefore, we analysed the average spine density and spine volume of neurons filled with Alexa 594 (**Figure 15 A**) from the uncaging experiment (section ***5.4***). We calculated spine density as the number of spines per 10 μm of dendritic length. We observed no difference in the average spine densities between control and prolonged CPA-treated CA1 pyramidal neurons (p-value = 0.814; unpaired Student's t test; n = 9 for control; n = 10 for CPA) (**Figure 15 B**). This suggests that the increase in mEPSC frequency is not due to an increase in number of spines, but most likely to a presynaptic effect (for example, an increase in release probability). As for the average spine volume, we did not observe a statistically significant difference between control and prolonged CPA-treated CA1 pyramidal neurons (p-value = 0.0968; unpaired Student's t test; n = 5 for control; n = 6 for CPA) (**Figure 15 C**). However, when all the spine volumes are plotted in a cumulative distribution curve, we observed a significant difference between the spine volumes of the two conditions (p-value < 0.001; two-sample K-S test) (**Figure 15 C**).

4.6 Spine localization of ER using pHluorin-GluA2 ΔC49

One feature of the store-operated response is the proximity of the ER membrane to the plasma membrane (around 10 nm). Normally, CA1 pyramidal neurons have very few spines invaded by ER (roughly 10-15% of spines) (Blumer *et al.*, 2015). Thus, the ER must invade spines in order to be in close enough proximity for the store-operated response to take place. To determine whether ER invades spines after prolonged calcium depletion or activity deprivation, cells were biolistically transfected with mCherry (morphology) and pHluorin-GluA2 ΔC49 (ER-retained). GluA2 ΔC49 is a truncated GluA2 subunit that remains in the ER (Greger *et al.*, 2002). Transfected CA1 pyramidal neurons were then imaged either after 2 days CPA (30 μM) treatment, 3 days TTX (1 μM) treatment, or no treatment (control) (**Figure 16 A**). The spine enrichment index was then calculated as shown in **Figure 16 B**. The average spine enrichment index was greater in CPA-treated than in control cells (p-value < 0.05; one-way ANOVA with post-hoc Tukey HSD test), greater in TTX-treated than in control cells (p-value < 0.05; one-way ANOVA with post-hoc Tukey HSD test), and was greater in TTX-treated than in CPA-treated cells (p-value < 0.05; one-way ANOVA with post-hoc Tukey HSD test) (n = 8 control; n = 9 for CPA; n = 10 for TTX) (**Figure 16 C**). When all the spine enrichment indices are plotted in a cumulative distribution curve, we observed a significant difference between the CPA-treated and the control cells (p-value < 0.001, ks test), the TTX-treated and the control cells (p-value < 0.001, ks test), and the TTX-treated and the CPA-treated cells (p-value < 0.001, ks test) (**Figure 16 C**). Thus, our data suggests that prolonged activity deprivation or ER-calcium store depletion both lead to a larger degree of spines invaded by ER.

4.7 Slow AHP in the presence of CPA

If TTX-induced HSP is a store-operated response, one assumption is that TTX leads to ER calcium store depletion. However, measuring calcium levels in the ER is not trivial. Therefore, we used the slow afterhyperpolarization (AHP) as a proxy for ER calcium levels. Briefly, the AHP is a phenomenon that refers to a hyperpolarisation that occurs after an action potential (fast AHP) or a series of action potentials (medium AHP, followed by slow AHP). The fast AHP lasts for about 2-5 ms and happens directly after an action potential. It is mediated by voltage- and calcium-activated potassium channels (big potassium channels: BK channels) (Matthews *et al*., 2009, Lee & Cui, 2010). The medium AHP lasts roughly 50-100 ms and happens after a train of action potentials. It is mediated by Ca^{2+}-gated potassium channels (small conductance calcium-activated potassium channels: SK channel family, SK1-4), predominantly the SK1 and SK2 channels (Villalobos *et al.*, 2004), and this current can be blocked by apamin (a selective SK channel blocker) (Hammond *et al*., 2006). There is also an apamin-insensitive component to the medium AHP that may be mediated by voltage-gated potassium channels (Kv7, the KCNQ family), but that are also Ca^{2+} mediated (Gu *et al.* 2005; Gu *et al.*, 2008; Tzingounis & Nicoll, 2008).

The slow AHP lasts for about 1-2 seconds and is elicited after a train of action potentials alongside the medium AHP. It is mediated by other forms of calcium-mediated potassium channels, different from those that underlie the fast and medium AHP. However, the identity of these channels is still unknown (Sah & Isaacson, 1995; Villalobos *et al*., 2004). One hypothesis states that the activation of the slow AHP current is indirectly calcium mediated, whereby increased calcium levels in the cytosol leads to an increase in membrane phosphatidylinositol 4,5-biphosphate levels, leading to the activation of the channels underlying the slow AHP current

(Andrade *et al*., 2012). KCNQ channels are also a possible candidate underlying the slow AHP current (Kim *et al.*, 2012). Regardless of the hypotheses behind the generation of the slow AHP, it is well established that it is a calcium-mediated potassium current.

Interestingly, the current of the slow AHP is largely dependent on calcium originating from internal stores. In other words, calcium induced calcium release (CICR) contributes to the slow AHP. As calcium rushes in to the cell after depolarization, this calcium opens ryanodine receptors located on the ER membrane, which causes the release of calcium from internal stores, which in turn contributes to the slow AHP. When CICR is blocked, the amplitude of the slow AHP is reduced (Torres *et al.*, 1996; Shah & Haylett, 2000; Qin *et al.*, 2012; Andrade *et al.*, 2012). This is especially true for CA1 pyramidal neuron, where CICR is found to contribute around 50% of the slow AHP current (**Figure 8**). Therefore, the slow AHP can be used as a proxy to assess relative calcium ER levels between various conditions. Therefore, we looked at the time course of slow AHP during states of low calcium store levels (**Figure 17**). To do this, we incubated organotypic hippocampal slices in CPA (30 μM) for 3 hours, recorded the AHP of CA1 pyramidal neurons in the presence of CPA, and compared the slow AHP amplitude with that of an untreated neuron (control). CPA was applied for 3 hours in order to be certain that ER calcium stores were depleted. The slow AHP was generated in voltage-clamp mode by holding the cell at -50 mV, depolarising the cell to 20 mV for 500 ms, and polarising the cell back to -50 mV. The depolarisation to 20 mV opens calcium channels, leading to the generation of calcium-mediated potassium currents underlying the AHP. We observed that in control cells, the slow AHP displays a run up, and maximises at around 60 seconds (**Figure 17 B**). The slow AHP is bigger in control cells than the acute CPA treated cells (p-value < 0.01; unpaired Student's t test; n = 11 for control; n = 9 for acute CPA) (**Figure 17 D**). Furthermore, when we compared the slow AHP at 0 seconds and at

60-90 seconds, we observed that the slow AHP increases at 60-90 seconds for control cells (p-value < 0.01; paired Student's t test; n = 11 for control at 0 seconds; n = 11 for control at 60-90 seconds), but not for the acute CPA-treated cells (p-value = 0.133; paired Student's t test; n = 9 for acute CPA at 0 seconds; n = 9 for acute CPA at 60-90 seconds). This is further shown in **Figure 17 C** where we compare the average difference (the slow AHP at 0 seconds subtracted from the slow AHP at 60-90 seconds) between the control and the acute CPA-treated cells (p-value < 0.01; unpaired Student's t test; n = 11 for control; n = 9 for acute CPA).

We also looked at the slow AHP after holding a CA1 pyramidal neuron at -70 mV for 5 minutes (**Figure 18**). This was to explore the possibility of the slow AHP decreasing after holding the cell at resting membrane potential as a result of ER calcium store depletion. After reaching a peak slow AHP, we stopped stimulating the cell for 5 minutes while holding it at -70 mV, then resumed the slow AHP protocol. **Figure 18 B** shows the time course of the experiment. When we compare the slow AHP at 120-140 seconds (peak slow AHP) and at 750 seconds (first stimulation after the 5 minute period at -70 mV), we observed that the slow AHP decreases at 750 seconds for control cells (p-value < 0.05; paired Student's t test; n = 10 for control at 120-140 seconds; n = 10 for control at 750 seconds), but not for the acute CPA-treated cells (p-value = 0.276; paired Student's t test; n = 8 for acute CPA at 120-140 seconds; n = 8 for acute CPA at 750 seconds). This is further shown in **Figure 18 C** where we compare the average difference (the slow AHP at 120-140 seconds subtracted from the slow AHP at 750 seconds) between the control and the acute CPA-treated cells (p-value < 0.01; unpaired Student's t test; n = 10 for control; n = 8 for acute CPA). Thus, our results suggest that the cell needs to be depolarised in order to refill its ER calcium stores, and that under resting membrane potential, the cell undergoes ER calcium store depletion.

5. Discussion

5.1 Prolonged ER calcium store depletion leads to an increase in the number of synaptic AMPA receptors

To determine whether AMPARs are governed by the store-operated response, we applied CPA (30 μM) on organotypic hippocampal slices for 24 or 48 hours, causing ER calcium stores to be depleted for a prolonged period of time. We chose this time scale in order to roughly match that of homeostatic synaptic plasticity by activity deprivation (TTX at 1 μM for 3 days) (Soares *et al.*, 2013). As stated previously, the 24 hour CPA treatment resulted in an average mEPSC amplitude that was borderline significantly larger than in control conditions (**Figure 10 B**). We then tried applying the same concentration of CPA for 48 hours to test whether the extended time of calcium store depletion would lead to a larger effect. We observed a significant increase in mEPSC amplitude for the 48 hour CPA treatment compared to control conditions. This increase in mEPSC amplitude suggests either the presence of a larger number of AMPA receptors at the synapse, a subunit change from GluA2-containing to GluA2-lacking AMPA receptors, or a combination of both. GluA2-lacking AMPA receptors have a larger conductance than the GluA2-containing variety which would lead to an increase in mEPSC amplitudes. As shown in **Figure 15 C**, spine volume seems to be increasing after prolonged calcium store depletion, suggesting the possibility of a larger population of AMPA receptors at synapses. These findings are interesting because the increase in synaptic strength is reminiscent of that seen during homeostatic synaptic plasticity.

For both 24 hour and 48 hour CPA treatments, no change was observed in the average mEPSC frequencies compared to control conditions, but the cumulative distribution of the inter-

event intervals between each mEPSC was left shifted. If the increase in frequency is real, it would suggest either a larger probability of spontaneous vesicular release, a larger number of synapses, or a combination of both. According to **Figure 15 B**, spine density seems unchanged after 48 hour CPA treatment, which highly suggests that the increase in frequency of mEPSCs would not be attributed to a larger number of synapses

Though these findings are fascinating, they could be due to the possibility that CPA treatment is affecting the activity of the network by dampening firing activity of the neurons. If so, then the observed effects can be attributed to decreased activity in the network, and this would be no different than the TTX treatment.

5.2 Acute CPA treatment has no effect on firing rate

To confirm that CPA application has no effect on the firing capacity of CA1 pyramidal neurons, we performed current injections in CA1 pyramidal neurons in control conditions and 3 hours after CPA application to be certain that ER calcium stores are depleted. The CPA-treated cells were recorded in the presence of CPA. As shown in **Figure 12 B**, CPA has no effect on the firing response patterns of CA1 pyramidal neurons. Therefore, the effects discussed in ***section 5.1*** are not due to decreased activity of the network, but most likely to the prolonged depletion of ER calcium stores.

5.3 Prolonged ER calcium store depletion leads to the insertion of GluA2-lacking AMPA receptors

Using stimulation-evoked AMPAR I-V curves in control and 48 hour CPA treatment, we observed a subunit switch from GluA2-containing to GluA2-lacking AMPA receptors. In other words, a prolonged period of calcium store depletion led to a shift in the synaptic AMPA receptor population from a calcium-impermeable to a calcium-permeable one. Interestingly, this change also happens at spines, dendritic shafts, and the soma as evidenced by glutamate uncaging evoked AMPAR I-V curves. This AMPA receptor subunit shift is also seen after prolonged activity deprivation (Béïque *et al.*, 2011; Soares *et al.*, 2013). This corroborates with the hypothesis of our first objective that prolonged depletion of ER calcium stores causes a shift from GluA2-containing to GluA2 lacking AMPARs. It is as though the cell is responding to calcium depletion by introducing a new source of calcium, which is consistent with the idea of a store-operated response. This however leads to the question of whether ER morphology is changing in order to favor a state which accommodates the process of calcium store-refilling. Enhanced synaptic strength and spine volume after prolonged CPA treatment led us to believe that the ER fills a larger number of spines after prolonged store depletion. ER-filled spines tend to be bigger and generate larger EPSCs than spines with no ER (Holbro *et al.*, 2009).

5.4 Prolonged ER calcium store depletion or activity deprivation leads to invasion of ER into dendritic spines

To determine whether ER invades spines after prolonged calcium depletion or activity deprivation, cells were biolistically transfected with mCherry (morphology) and pHluorin-GluA2 ΔC49 (ER-retained). The pHluorin-GluA2 ΔC49 construct is a cleaved AMPA receptor that remains trapped in the ER (Rathje *et al.*, 2013). Normally, CA1 pyramidal neurons have very few spines invaded by ER (roughly 10-15% of spines) (Blumer *et al.*, 2015), and the store-operated response requires the ER to be within 10 nm of the plasma membrane (Alonso *et al.*, 2012). Therefore, we expect a larger amount of ER-filled spines after 48 hour CPA (30 μM) treatment and 72 hour TTX (1 μM) treatment. Using the spine enrichment index, we observed that TTX-treated neurons had the most ER invasion of spines, followed by the CPA treated neurons, and lastly, the control neurons.

Firstly, this suggests that activity deprivation and prolonged calcium store depletion lead to the same fate, which is a compensatory mechanism in order to return ER calcium levels within an optimal range. As the ER invades spines, they are closer to GluA2-lacking AMPA receptors, which is one of the requirements for a store-operated response. Secondly, TTX-treated slices seem to have a higher degree of ER invasion than in CPA. This can be attributed to either ER calcium depletion being only partly responsible for the effects seen in homeostatic synaptic plasticity, or that the 48 hour CPA time point is too short to reach the state of the 72 hour TTX treatment. Different time points for the CPA treatment (including the 72 hour CPA treatment) are needed in order to distinguish between the two possible reasons for this discrepancy. Furthermore, electron microscopy is needed to confirm whether the ER that invades spines after treatment is within the

critical distance (around 10 nm) from the spine plasma membrane to undergo the store-operated response. Overall these data corroborates our hypothesis that HSP induced by TTX and the store-operated response act through the same mechanism. However, an occlusion experiment comparing control neurons to CPA treated, TTX treated, and CPA+TTX treated neurons would shed more light on whether HSP induced by TTX and the store-operated response operate through a common pathway.

5.5 CA1 pyramidal neurons' ER calcium stores are depleted within 5 minutes at resting membrane potential

Our second hypothesis that HSP induced by TTX and the store-operated response act through the same mechanism comes with the assumption that TTX treatment leads to calcium store depletion. Under resting membrane potential, central neurons (including CA1 pyramidal neurons) have a very low level of ER calcium, and this is only replenished by depolarizing the cell to open voltage-gated calcium channels (Shmigol *et al.*, 1994) (**Figure 19**). Furthermore, ER calcium stores of CA1 pyramidal neurons empty within 5 minutes of CPA application in CA1 neurons from dissociated cultures (Samtleben *et al.*, 2013; Shmigol *et al.*, 1994). Here, we use the slow AHP as a proxy to measure the level of calcium in the ER. First, we checked if CPA treatment blocked part of the slow AHP (**Figure 17**). As expected, roughly 50% of the slow AHP was blocked with acute CPA treatment (**Figure 17 D**). Interestingly a large run-up of the slow AHP was observed in control neurons (**Figure 17 E**), but not in the acute CPA treated neurons (**Figure 17 F**). If the ER is normally at a low level in CA1 hippocampal neurons, then this run-up could be seen as the cell refilling its ER stores. The slow AHP is generated in voltage-clamp mode by holding the cell at -

50 mV, depolarising the cell to 20 mV for 500 ms, and polarising the cell back to -50 mV. The depolarisation to 20 mV opens calcium channels, leading to the generation of calcium-mediated potassium currents underlying the AHP. In the initial stimulation of the slow AHP, this calcium current may possibly be used not just for the generation of the slow AHP, but also the refilling of the ER stores, which subsequently leads to larger slow AHP as the contribution of CICR increases. If this were the case, then holding a CA1 pyramidal neuron at -70 mV for 5 minutes should cause the slow AHP in control conditions to reduce back to its initial state, whereas the acute CPA-treated cells should have an unchanged slow AHP (**Figure 18**). As hypothesised, the slow AHP in control conditions returns to its initial state, and this drop in slow AHP amplitude is blocked by acute CPA treatment (**Figure 18 B-E**). This shows that CA1 pyramidal neurons, under resting membrane potential, has low calcium levels, which are rapidly depleted (within 5 minutes). This suggests that prolonged TTX treatment or activity deprivation leads to a state where CA1 pyramidal neuron are depolarised a lot less, leading to a state of low ER calcium across a long period of time, as opposed to neurons where activity is not perturbed. It seems that taking away action potential firing is equivalent to hindering the store-refilling mechanism of the neuron. Therefore, CA1 neurons respond to this prolonged activity deprivation by increasing calcium conductance through GluA2-lacking AMPA receptors in order to compensate for the reduced number of open voltage-gated calcium channels.

6. Conclusion

Collectively, the data highly suggests that the regulation of a population of glutamate receptor subunits is part of the store-operated response in central neurons. Furthermore, the data corroborates the idea that HSP induced by TTX and the store-operated response may, in fact, act through the same mechanism. **Figure 20** represents the model supported by the data. Within the model (**Figure 20**), STIM-1 is poised as a prime candidate for the sensor of HSP as it is also the sensor for the store-operated response. To investigate this, we will biolistically transfect organotypic hippocampal slices with a STIM-1 shRNA in order to observe the effects of homeostatic synaptic plasticity in the absence of STIM-1. Either the cell cannot sense it has low ER calcium (no change in AMPA receptor population with TTX treatment), it assumes it is always in a state of low calcium (transfected neurons express GluA2-lacking AMPA receptors without TTX or CPA), or the mechanism is STIM-1 independent. Either way, it would shed light on whether HSP is, in essence, a store-operated response.

It is largely believed that Hebbian plasticity is the fundamental mechanism underlying the way the brain stores information and mediates learning. We also know that Hebbian plasticity can modulate synaptic strength by up- or down-regulating AMPARs at synapses. Furthermore, HSP has been shown to be able to also modulate the expression of AMPARs. We can therefore deduce that HSP may also be an important mechanism in brain information coding. If HSP is shown to be, at least in part, a store-operated response, then the mechanism underlying HSP would be exposed to be tightly linked with levels of internal Ca^{2+} stores. In fact, the importance of ER in HSP has already been alluded in synaptopdin (SP)-deficient mice lacking the spine apparatus (SA) – an organelle in the spine composed of stacked smooth ER. The granule cells of these mice were

unable to be synaptically potentiated by denervation-induced synaptic scaling as opposed to granule cells of wild-type mice. Furthermore TTX-induced HSP led to an increase in mEPSC in wild type granule cells, but not in SP-deficient ones (Vlachos *et al.*, 2013). This finding reveals the necessity of ER in HSP, but lacks any mechanistic explanation for its existence in this process. My data however sheds some light on the mechanism behind HSP, putting ER Ca^{2+} as a possible signalling ion for this phenomenon, presumably acting through STIM-1 interaction. Thus, elucidating the functional role of ER Ca^{2+} stores on synaptic transmission would shed light on the fundamental mechanisms and principles underlying the ability of the brain to store and process information and learn.

References

Abbott, L.F., & Nelson, S.B. (2000). Synaptic plasticity: taming the beast. *Nat Neurosci 3 Suppl*, 1178-1183.

Abraham, W.C. (2003). How long will long-term potentiation last?. *Philos Trans R Soc Lond B Biol Sci 358*, 735-744.

Alonso, M.T., Manjarrés, I.M., García-Sancho, J. (2012). Privileged coupling between Ca(2+) entry through plasma membrane store-operated Ca(2+) channels and the endoplasmic reticulum Ca(2+) pump. *Mol Cell Endocrinol 353*, 37-44.

Andrade, R., Foehring, R. C., & Tzingounis, A. V. (2012). The calcium-activated slow AHP: cutting through the Gordian knot. *Front Cell Neurosci 6*, 47.

Béïque, J.C., Lin, D.T., Kang, M.G., Aizawa, H., Takamiya, K., & Huganir, R.L. (2006). Synapse-specific regulation of AMPA receptor function by PSD-95. *Proc Natl Acad Sci U S A 103*, 19535-19540.

Béïque, J.C., Na, Y., Kuhl, D., Worley, P.F., & Huganir, R.L. (2011). Arc-dependent synapse-specific homeostatic plasticity. *Proc Natl Acad Sci U S A 108*, 816-821.

Bi, G.Q., & Poo, M.M. (1998). Synaptic modifications in cultured hippocampal neurons: dependence on spike timing, synaptic strength, and postsynaptic cell type. *J Neurosci 18*, 10464-10472.

Blumer, C., Vivien, C., Genoud,C., Perez-Alvarez, A., Wiegert, J.S., Vetter, T., Oertner, T.G. (2015). Automated analysis of spine dynamics on live CA1 pyramidal cells. *Med Image Anal 1*, 87-97.

Bowie, D., & Mayer, M.L. (1995). Inward rectification of both AMPA and kainate subtype glutamate receptors generated by polyamine-mediated ion channel block. *Neuron 15*, 453-462.

Cahalan, M.D., Zhang, S.L., Yeromin, A.V., Ohlsen, K., Roos, J., Stauderman, K.A. (2007). Molecular basis of the CRAC channel. *Cell Calcium 42*, 133-144.

Cannon, W.B., & Rosenblueth, A. (1949). *The supersensitivity of denervated structure*. New York: Macmillan.

Collingridge, G.L., Kehl, S.J., & McLennan, H. (1983). The antagonism of amino acid-induced excitations of rat hippocampal CA1 neurones in vitro. *J Physiol 334*, 19-31.

Cull-Candy, S.G., & Leszkiewicz, D.N. (2004). Role of distinct NMDA receptor subtypes at central synapses. *Sci STKE 2004*, re16.

Davis, G.W. (2006). Homeostatic control of neural activity: from phenomenology to molecular design. *Annu Rev Neurosci 29*, 307-323.

Deeg, K.E., & Aizenman, C.D., (2011). Sensory modality-specific homeostatic plasticity in the developing optic tectum. *Nat Neurosci 14*, 548-550.

Desai, N.S., Cudmore, R.H., Nelson, S.B., & Turrigiano, G.G. (2002). Critical periods for experience-dependentsynapticscalinginvisualcortex. *Nat Neurosci 5*, 783-789.

Ding, Y.X., Zhang, Y., He, B., Yue, W.H., Zhang, D., & Zou, L.P. (2010). A possible association of responsiveness to adrenocorticotropic hormone with specific GRIN1 haplotypes in infantile spasms. *Dev Med Child Neurol 52*, 1028-1032.

Dingledine, R., Borges, K., Bowie, D., & Traynelis, S.F. (1999). The glutamate receptor ion channels. *Pharmacol Rev 51*, 7-61.

Endele, S., Rosenberger, G., Geider, K., Popp, B., Tamer, C., Stefanova, I., et al. (2010). Mutations in GRIN2A and GRIN2B encoding regulatory subunits of NMDA receptors cause variable neurodevelopmental phenotypes. *Nat Genet 42*, 1021-1026.

Feldman, D.E. (2000). Timing-based LTP and LTD at vertical inputs to layer II/III pyramidal cells in rat barrel cortex. *Neuron 27*,45-56.

Forrest, D., Yuzaki, M., Soares, H.D., Ng, L., Luk, D.C., Sheng, M., et al. (1994). Targeted disruption of NMDA receptor 1 gene abolishes NMDA response and results in neonatal death. *Neuron 13*, 325-338.

Furukawa, H., & Gouaux, E. (2003). Mechanisms of activation, inhibition and specificity: crystal structures of the NMDA receptor NR1 ligand-binding core. *EMBO J 22*, 2873-2885.

Furukawa, H., Singh, S.K., Mancusso, R., & Gouaux, E. (2005). Subunit arrangement and function in NMDA receptors. *Nature 438*, 185-192.

Gao, M., Sossa, K., Song, L., Errington, L., Cummings, L., Hwang, H., Kuhl, D., Worley, P., & Lee, H.K. (2010). A specific requirement of Arc/Arg3.1 for visual experience-induced homeostatic synaptic plasticity in mouse primary visual cortex. *J Neurosci 30*, 7168-7178.

Goel, A., Jiang, B., Xu, L.W., Song, L., Kirkwood, A., & Lee, H.K. (2006). Cross-modal regulation of synaptic AMPA receptors in primary sensory cortices by visual experience. *Nat Neurosci 9*, 1001-1003.

Goel, A., Lee, H.K., 2007. Persistence of experience-induced homeostatic synaptic plasticity through adulthood in superficial layers of mouse visual cortex. J. Neurosci. 27, 6692-6700.

Goold, C.P., Nicoll, R.A. (2010). Single-cell optogenetic excitation drives homeostatic synaptic depression. *Neuron 68*, 512-528.

Greger, I.H., Khatri, L., & Ziff, E.B. (2002). RNA editing at arg607 controls AMPA receptor exit from the endoplasmic reticulum. *Neuron 34*, 759-772.

Groth, R.D., Lindskog, M., Thiagarajan, T.C., Li, L., & Tsien, R.W. (2011). Beta Ca^{2+}/CaM-dependent kinase type II triggers upregulation of GluA1 to coordinate adaptation to synaptic inactivity in hippocampal neurons. *Proc Natl Acad Sci U S A 108*, 828-833.

Gu, N., Hu, H., Vervaeke, K., & Storm, J. F. (2008). SK (KCa2) channels do not control somatic excitability in CA1 pyramidal neurons but can be activated by dendritic excitatory synapses and regulate their impact. *J Neurophysiol, 100*, 2589-2604

Gu, N., Vervaeke, K., Hu, H., & Storm, J. F. (2005). Kv7/KCNQ/M and HCN/h, but not KCa2/SK channels, contribute to the somatic medium after-hyperpolarization and excitability control in CA1 hippocampal pyramidal cells. *J Physiol, 566*(Pt 3), 689-715.

Hammond, R. S., Bond, C. T., Strassmaier, T., Ngo-Anh, T. J., Adelman, J. P., Maylie, J., & Stackman, R. W. (2006). Small-conductance Ca2+-activated K+ channel type 2 (SK2) modulates hippocampal learning, memory, and synaptic plasticity. *J Neurosci, 26*, 1844-1853.

Hebb, D.O. (1949). The organization of behavior: a neuropsychological theory. New York: Wiley.

Holbro, N., Grunditz, A., & Oertner, T.G. (2009). Differential distribution of endoplasmic reticulum controls metabotropic signaling and plasticity at hippocampal synapses. *Proc Natl Acad Sci U S A 35*, 15055-15060.

Horak, M., & Wenthold, R.J. (2009). Different roles of C-terminal cassettes in the trafficking of full-length NR1 subunits to the cell surface. *J Biol Chem 284*, 9683-9691.

Houweling, A.R., Bazhenov, M., Timofeev, I., Steriade, M., & Sejnowski, T.J. (2005). Homeostatic synaptic plasticity can explain post-traumatic epileptogenesis in chronically isolated neocortex. *Cereb Cortex 15*, 834-845.

Ibata, K., Sun, Q., & Turrigiano, G.G. (2008). Rapid synaptic scaling induced by changes in postsynaptic firing. *Neuron 57*, 819-826.

Johnson, J.W., & Ascher, P. (1987). Glycine potentiates the NMDA response in cultured mouse brain neurons. *Nature 325*, 529-531.

Kandel, E.R., Schwartz, J.H., & Jessel, T.M. (2000). Principles of Neural Science, 4th Edition. New York: McGraw-Hill.

Kerchner, G.A., & Nicoll, R.A. (2008). Silent synapses and the emergence of a postsynaptic mechanism for LTP. *Nat Rev Neurosci 9*, 813-825.

Kessels, H.W. & Malinow, R. (2009). Synaptic AMPA receptor plasticity and behavior. *Neuron 61*, 340-350.

Kim, K. S., Kobayashi, M., Takamatsu, K., & Tzingounis, A. V. (2012). Hippocalcin and KCNQ channels contribute to the kinetics of the slow afterhyperpolarization. *Biophys J 103*, 2446-2454.

Kleckner, N.W., & Dingledine, R. (1988). Requirement for glycine in activation of NMDA-receptors expressed in Xenopus oocytes. *Science 241*, 835-837.

Kotak, V.C., Fujisawa, S., Lee, F.A., Karthikeyan, O., Aoki, C., & Sanes, D.H. (2005). Hearing loss raises excitability in the auditory cortex. *J Neurosci 25*, 3908-3918.

Krestel, H.E., Shimshek, D.R., Jensen, V., Nevian, T., Kim, J., Geng, Y., et al. (2004). A genetic switch for epilepsy in adult mice. *J Neurosci 24*, 10568-10578.

Lazar, A., Pipa, G., & Triesch, J. (2009). SORN: a self-organizing recurrent neural network. *Front Comput Neurosci 3*, 23.

Lee, K.F., Soares, C., Béïque, J.C. (2014). Tuning into diversity of homeostatic synaptic plasticity. *Neuropharmacology 78*, 31-37.

Lee, U. S., & Cui, J. (2010). BK channel activation: structural and functional insights. *Trends Neurosci, 33*, 415-423.

Lerma, J., Zukin, R.S., & Bennett, M.V. (1990). Glycine decreases desensitization of N-methyl-D-aspartate (NMDA) receptors expressed in Xenopus oocytes and is required for NMDA responses. *Proc Natl Acad Sci USA 87*, 2354-2358.

Lindskog, M., Li, L., Groth, R.D., Poburko, D., Thiagarajan, T.C., Han, X., & Tsien, R.W. (2011). Postsynaptic GluA1 enables acute retrograde enhancement of presynaptic function to coordinate adaptation to synaptic inactivity. *Proc Natl Acad Sci U S A 107*, 21806-21811.

Lisman, J., & Raghavachari, S. (2006). A unified model of the presynaptic and postsynaptic changes during LTP at CA1 synapses. *Sci STKE 2006*, re11.

Lu, W., Shi, Y., Jackson, AC., Bjorgan, K., During, M.J., et al. (2009). Subunit composition of synaptic AMPA receptors revealed by a single-cell genetic approach. *Neuron 62*, 254-268.

Luik, R.M., Wu, M.M., Buchanan, J., Lewis, R.S. (2006). The elementary unit of store-operated Ca^{2+} entry: local activation of CRAC channels by STIM1 at ER-plasma membrane junctions. *J Cell Biol 174*, 815-825

Lynch, G., Larson, J., Kelso, S., Barrionuevo, G., & Schottler, F. (1983). Intracellular injections of EGTA block induction of hippocampal long-term potentiation. *Nature 305*, 719-721.

Malenka, R.C., & Nicoll, R.A. (1999). Long-term potentiation--a decade of progress? *Science 285*, 1870-1874.

Malenka, R.C., & Bear, M.F. (2004). LTP and LTD: an embarrassment of riches. *Neuron 44*, 5-21.

Malinow, R., Madison, D.V., & Tsien, R.W. (1988). Persistent protein kinase activity underlying long-term potentiation. *Nature 335*, 820-824.

Malinow, R., Schulman, H., & Tsien, R.W. (1989). Inhibition of postsynaptic PKC or CaMKII blocks induction but not expression of LTP. *Science 245*, 862-866.

Malinow, R., & Malenka, R.C. (2002). AMPA receptor trafficking and synaptic plasticity. *Annu Rev Neurosci 25*, 103-126.

Markram, H., Lubke, J., Frotscher, M., & Sakmann, B. (1997). Regulation of synaptic efficacy by coincidence of postsynaptic APs and EPSPs. *Science 275*, 213-215.

Mathern, G.W., Pretorius, J.K., Leite, J.P., Kornblum, H.I., Mendoza, D., Lozada, A., et al. (1998). Hippocampal AMPA and NMDA mRNA levels and subunit immunoreactivity in human temporal lobe epilepsy patients and a rodent model of chronic mesial limbic epilepsy. *Epilepsy Res 32*, 154-171.

Mateos-Aparicio, P., Murphy, R., & Storm, J. F. (2014). Complementary functions of SK and Kv7/M potassium channels in excitability control and synaptic integration in rat hippocampal dentate granule cells. *J Physiol 592*(Pt 4), 669-693.

Mayer, M.L., Westbrook, G.L., & Guthrie, P.B. (1984). Voltage-dependent block by Mg^{2+} of NMDA responses in spinal cord neurones. *Nature 309*, 261-263.

Miller, K.D., & MacKay, D.J. (1994). The Role of Constraints in Hebbian Learning. *Neural Comput 6*, 100-126.

Moncoq, K., Trieber, C.A., & Young, H.S. (2007). The Molecular Basis for Cyclopiazonic Acid Inhibition of the Sarcoplasmic Reticulum Calcium Pump. *J Biol Chem 282*, 9748-9757

Monyer, H., Sprengel, R., Schoepfer, R., Herb A., Higuchi M., Lomeli H., et al. (1992). Heteromeric NMDA receptors: molecular and functional distinction of subtypes. *Science 256*, 1217-1221.

Monyer, H., Burnashev, N., Laurie, D.J., Sakmann, B., & Seeburg, P.H. (1994). Developmental and regional expression in the rat brain and functional properties of four NMDA receptors. *Neuron 12*, 529-540.

Nowak, L., Bregestovski, P., Ascher, P., Herbet, A., & Prochiantz, A. (1984). Magnesium gates glutamate-activated channels in mouse central neurones. *Nature 307*, 462-465.

O'Brien, R.J., Kamboj, S., Ehlers, M.D., Rosen, K.R., Fischbach, G.D., & Huganir, R.L. (1998). Activity-dependent modulation of synaptic AMPA receptor accumulation. *Neuron 21*, 1067-1078.

Perez-Otano, I., & Ehlers, M.D. (2005). Homeostatic plasticity and NMDA receptor trafficking. *Trends Neurosci 28*, 229-238.

Qin, Z., Zhou, X., Gomez-Smith, M., Pandey, N.R., Lee, K.F., Lagace, D.C., Béïque, J.C., & Chen, H.H. (2012). LIM domain only 4 (LMO4) regulates calcium-induced calcium release and synaptic plasticity in the hippocampus. *J Neurosci 32*, 4271-4283.

Rathje, M., Fang, H., Bachman, J.L., Anggono, V., Gether, U., Huganir, R.L., Madsen, K.L. (2013). AMPA receptor pHluorin-GluA2 reports NMDA receptor-induced intracellular acidification in hippocampal neurons. *Proc Natl Acad Sci U S A 35*, 14426-14431.

Roos, J., DiGregorio, P.J., Yeromin, A.V., Ohlsen, K., Lioudyno, M., Zhang, S., Safrina, O., Kozak, J.A., Wagner, S.L., Cahalan, M.D., Veliçelebi, G., Stauderman, K.A. (2005). STIM1, an essential and conserved component of store-operated Ca^{2+} channel function. *J Cell Biol 169*, 435-445.

Samtleben, S., Jaepel, J., Fecher, C., Andreska, T., Rehberg, M., & Blum, R. (2013). Direct imaging of ER calcium with targeted-esterase induced dye loading (TED). *J Vis Exp 7*, e50317.

Sah, P., & Isaacson, J. S. (1995). Channels underlying the slow afterhyperpolarization in hippocampal pyramidal neurons: neurotransmitters modulate the open probability. *Neuron 15*, 435-441.

Sanchez, R.M., Koh, S., Rio, C., Wang, C., Lamperti, E.D., Sharma, D., et al. (2001). Decreased glutamate receptor 2 expression and enhanced epileptogenesis in immature rat hippocampus after perinatal hypoxia-induced seizures. *J Neurosci 21*, 8154-8163.

Schorge, S., & Colquhoun, D. (2003). Studies of NMDA receptor function and stoichiometry with truncated and tandem subunits. *J Neurosci 23*, 1151-1158.

Seeburg, P.H., & Hartner, J. (2003). Regulation of ion channel/neurotransmitter receptor function by RNA editing. *Curr Opin Neurobiol 13*, 279-283.

Shah, M., & Haylett, D. G. (2000). Ca(2+) channels involved in the generation of the slow afterhyperpolarization in cultured rat hippocampal pyramidal neurons. *J Neurophysiol 83*, 2554-2561.

Shepherd, J.D., & Huganir, R.L. (2007). The cell biology of synaptic plasticity: AMPA receptor trafficking. *Annu Rev Cell Dev Biol 23*, 613-643.

Sjostrom, P.J., Turrigiano, G.G., & Nelson, S.B. (2001). Rate, timing, and cooperativity jointly determine cortical synaptic plasticity. *Neuron 32*, 1149-1164.

Smigol, A., Kirischuk, S., Kostyuk, P., & Verkhratsky, A. (1994). Different properties of caffeine-sensitive Ca^{+} stores in peripheral and central mammalian neurones. *European Journal of Phyiology 426*, 174-176.

Soares, C., Lee K.F., Nassrallah, W., & Béïque J.C. (2013). Differential subcellular targeting of glutamate receptor subtypes during homeostatic synaptic plasticity. *J Neurosci 33*, 13547-13559

Soares, C., Lee K.F., Cook, D., & Béïque J.C. (2013). A cost-effective method for preparing, maintaining, and transfecting neurons in organotypic slices. *Methods Mol Biol 1183*, 205-219.

Soden, M.E., & Chen, L. (2010). Fragile X protein FMRP is required for homeostatic plasticity and regulation of synaptic strength by retinoic acid. *J Neurosci 30*, 16910-16921.

Sommer, B., Kohler, M., Sprengel, R., & Seeburg, P.H. (1991). RNA editing in brain controls a determinant of ion flow in glutamate-gated channels. *Cell 67*, 11-19.

Spruston, N. (2008). Pyramidal neurons: dendritic structure and synaptic integration. *Nat Rev Neurosci 9*, 206-221.

Stoppini, L., Buchs P.A., & Muller D. (1991). A simple method for organotypic cultures of nervous tissue. *J Neurosci Methods 37*, 173-182.

Sutton, M.A., Ito, H.T., Cressy, P., Kempf, C., Woo, J.C., & Schuman, E.M. (2006). Miniature neurotransmission stabilizes synaptic function via tonic suppression of local dendritic protein synthesis. *Cell 125*, 785-799.

Tanaka, H., Grooms, S.Y., Bennett, M.V., & Zukin, R.S. (2000). The AMPAR subunit GluR2: still front and center-stage. *Brain Res 886*, 190-207.

Thivierge, J.P., & Cisek, P. (2008). Nonperiodic synchronization in heterogeneous networks of spiking neurons. *J Neurosci 28*, 7968-7978.

Torres, G. E., Arfken, C. L., & Andrade, R. (1996). 5-Hydroxytryptamine4 receptors reduce afterhyperpolarization in hippocampus by inhibiting calcium-induced calcium release. *Mol Pharmacol 50*, 1316-1322.

Toyoizumi, T., Pfister, J.P., Aihara, K., & Gerstner, W. (2005). Generalized Bienenstock-Cooper-Munro rule for spiking neurons that maximizes information transmission. *Proc Natl Acad Sci U S A 102*, 5239-5244.

Traynelis, S.F., Wollmuth, L.P., McBain, C.J., Menniti, F.S., Vance, K.M., Ogden, K.K., et al. (2010). Glutamate receptor ion channels: structure, regulation, and function. *Pharmacol Rev 62*, 405-496.

Kim, J., Tsien, R.W., 2008. Synapse-specific adaptations to inactivity in hippocampal circuits achieve homeostatic gain control while dampening network reverberation. *Neuron 58*, 925-937.

Turrigiano, G.G., Leslie, K.R., Desai, N.S., Rutherford, L.C., & Nelson, S.B. (1998). Activity-dependent scaling of quantal amplitude in neocortical neurons. *Nature 391*, 892-896.

Turrigiano, G.G., & Nelson, S.B. (2004). Homeostatic plasticity in the developing nervous system. *Nat Rev Neurosci 5*, 97-107.

Turrigiano, G.G. (2008). The self-tuning neuron: synaptic scaling of excitatory synapses. *Cell 135*, 422-435.

Turrigiano, G. (2011). Too many cooks? Intrinsic and synaptic homeostatic mechanisms in cortical circuit refinement. *Annu Rev Neurosci 34*, 89-103.

Turrigiano, G. (2012). Homeostatic synaptic plasticity: local and global mechanisms for stabilizing neuronal function. *Cold Spring Harb Perspect Biol 4*, a005736.

Tzingounis, A. V., & Nicoll, R. A. (2008). Contribution of KCNQ2 and KCNQ3 to the medium and slow afterhyperpolarization currents. *Proc Natl Acad Sci U S A 105*, 19974-19979.

Ulbrich, M.H., & Isacoff, E.Y. (2007). Subunit counting in membrane-bound proteins. *Nat Methods 4*, 319-321.

Ulbrich, M.H., & Isacoff, E.Y. (2008). Rules of engagement for NMDA receptor subunits. *Proc Natl Acad Sci USA 105*, 14163-14168.

Vlachos, A., Ikenberg, B., Lenz, M., Becker, D., Reifenberg, K., Bas-Orth, C., & Deller, T. (2013). Synaptopodin regulates denervation-induced homeostatic synaptic plasticity. *Proc Natl Acad Sci U S A 110*, 8242-8247.

Villalobos, C., Shakkottai, V. G., Chandy, K. G., Michelhaugh, S. K., & Andrade, R. (2004). SKCa channels mediate the medium but not the slow calcium-activated afterhyperpolarization in cortical neurons. *J Neurosci 24*, 3537-3542.

Whitlock, J.R., Heynen, A.J., Shuler, M.G., & Bear, M.F. (2006). Learning induces long-term potentiation in the hippocampus. *Science 313*, 1093-1097.

Whitt, J.L., Petrus, E., & Lee, H.K. (2014). Experience-dependent homeostatic synaptic plasticity in neocortex. *Neuropharmacology 78*, 45-54.

Wong, M. (2005). Advances in the pathophysiology of developmental epilepsies. *Semin Pediatr Neurol 12*, 72-87.

Yao, Y., Harrison, C.B., Freddolino, P.L., Schulten, K., & Mayer, M.L. (2008). Molecular mechanism of ligand recognition by NR3 subtype glutamate receptors. *EMBO J 27*, 2158-2170.

Yeung, L.C., Shouval, H.Z., Blais, B.S., & Cooper, L.N. (2004). Synaptic homeostasis and input selectivity follow from a calcium-dependent plasticity model. *Proc Natl Acad Sci U S A 101*, 14943-14948.

Yu, X., Chung, S., Chen, D.Y., Wang, S., Dodd, S.J., Walters, J.R., Isaac, J.T., & Koretsky, A.P. (2012). Thalamocortical inputs show post-critical-period plasticity. *Neuron 74*, 731-742.

Annexe

Introduction Figures

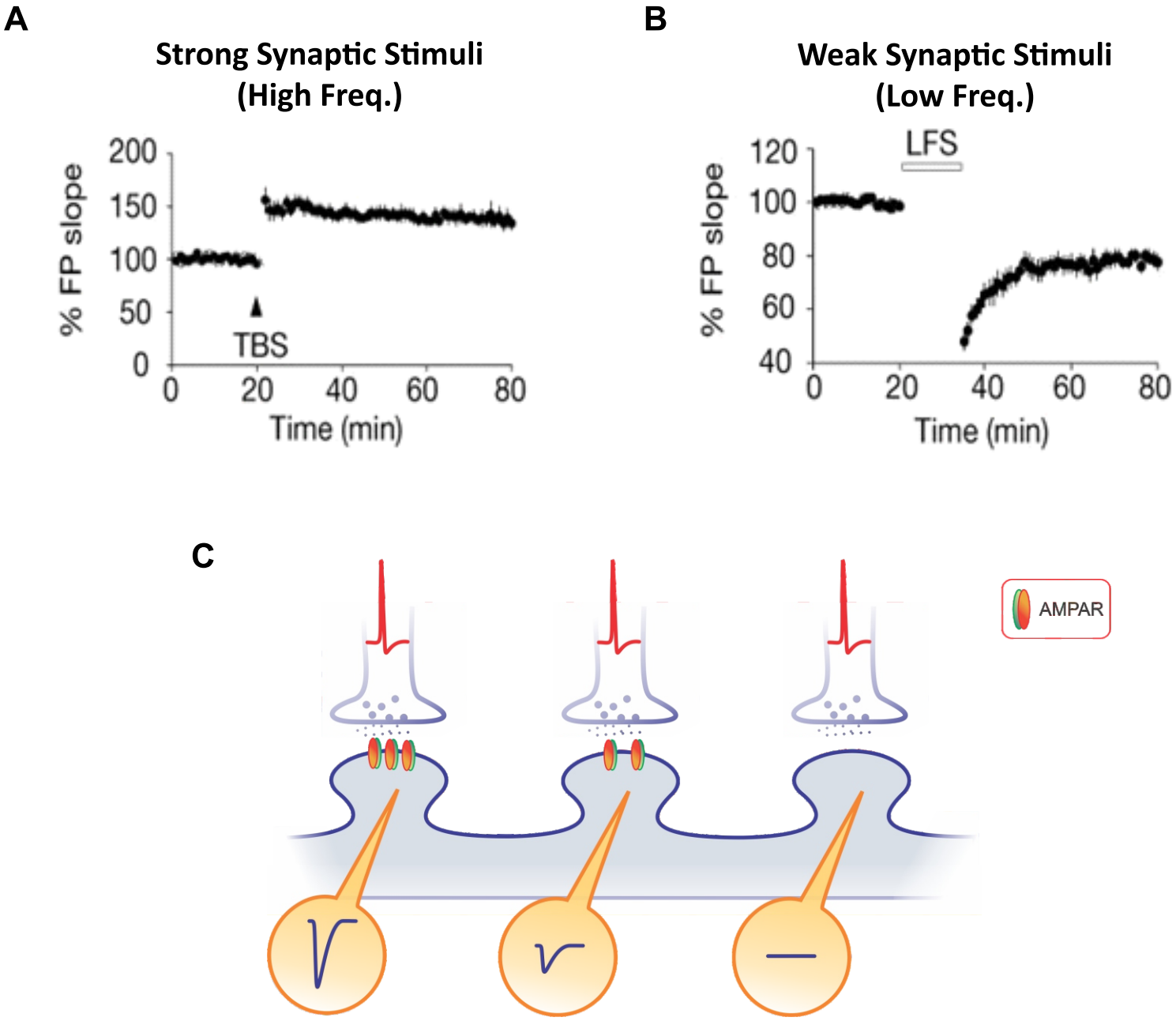

Figure 1. Hebbian Plasticity. **A**, Long Term Potentiation (LTP) is a long-term enhancement of signal transmission between two neurons as a result of a high frequency stimulation of the presynaptic neuron. **B**, Long Term Depression (LTD)is a long-term decrease in the efficacy of signal transmission between two neurons due to low frequency stimuli. **C**, Synaptic strength correlates with the number of AMPA receptors at the synapse.

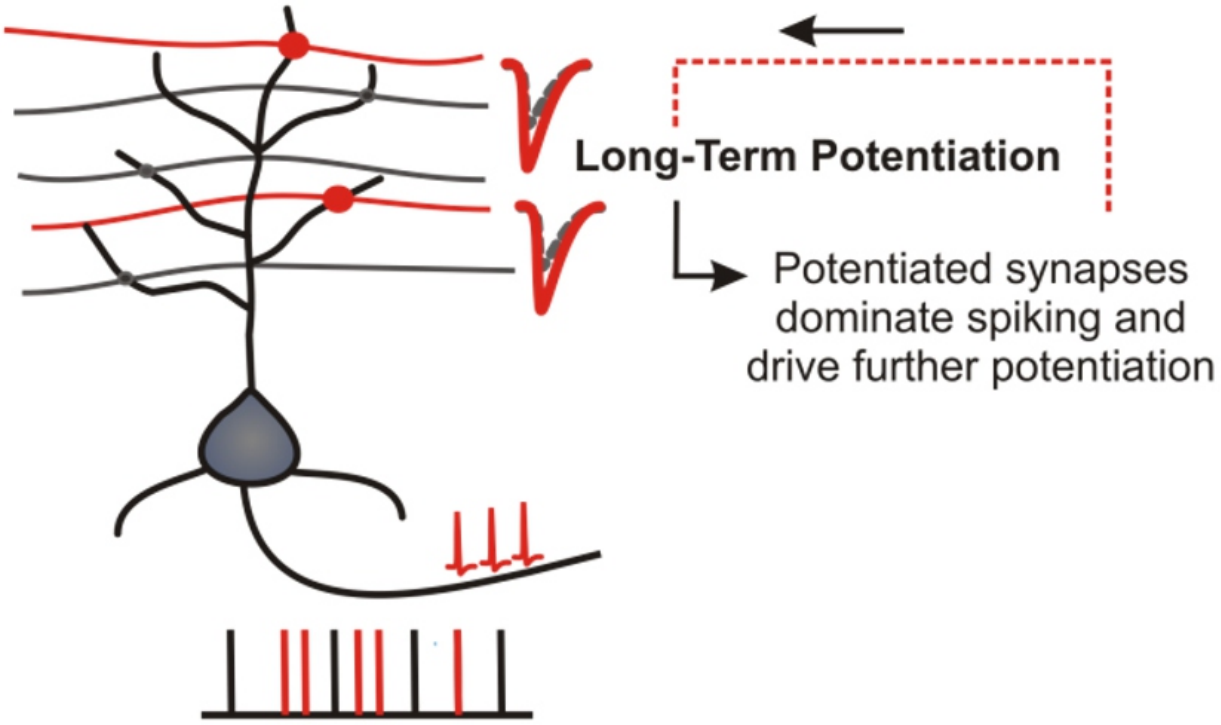

Figure 2. Problems with models that solely implement Hebbian plasticity (in this case, LTP). Synapses are driven to an excess of potentiation, causing some synapses to reach a functional plateau. These positive-feedback processes may lead to the development of epileptogenic activity in neurons (Turrigiano & Nelson, 2004).

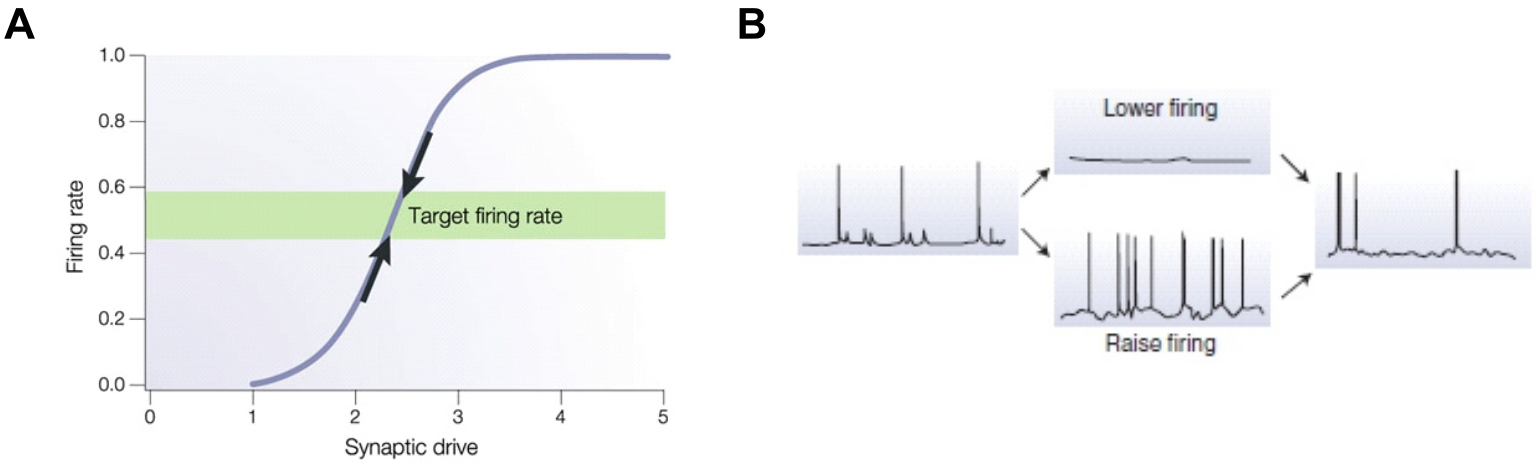

Figure 3. Homeostatic Plasticity. **A**, Neurons can keep their spiking activity within an ideal range, and therefore play the role of stable carriers of information in brain activity (Turrigiano & Nelson, 2004). **B**, When activity in a network is artificially raised or lowered for a prollonged period of time, neurons find a way to regain their previous firing rate (Turrigiano, 2012).

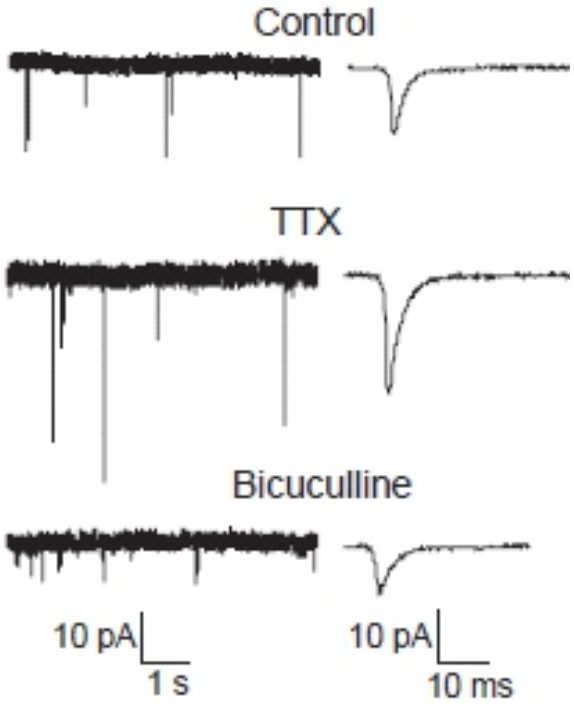

Figure 4. Homeostatic Synaptic Plasticity (HSP). On one hand, the prolonged reduction of a neuron's firing activity leads to the reinforcement of its excitatory synapses (TTX. voltage-gated sodium channel blocker). On the other, the prolonged enhancement of its firing activity results in the weakening of its excitatory synapses (Bicuculline, GABAA receptor antagonist). (Turrigiano *et al.*, 1998).

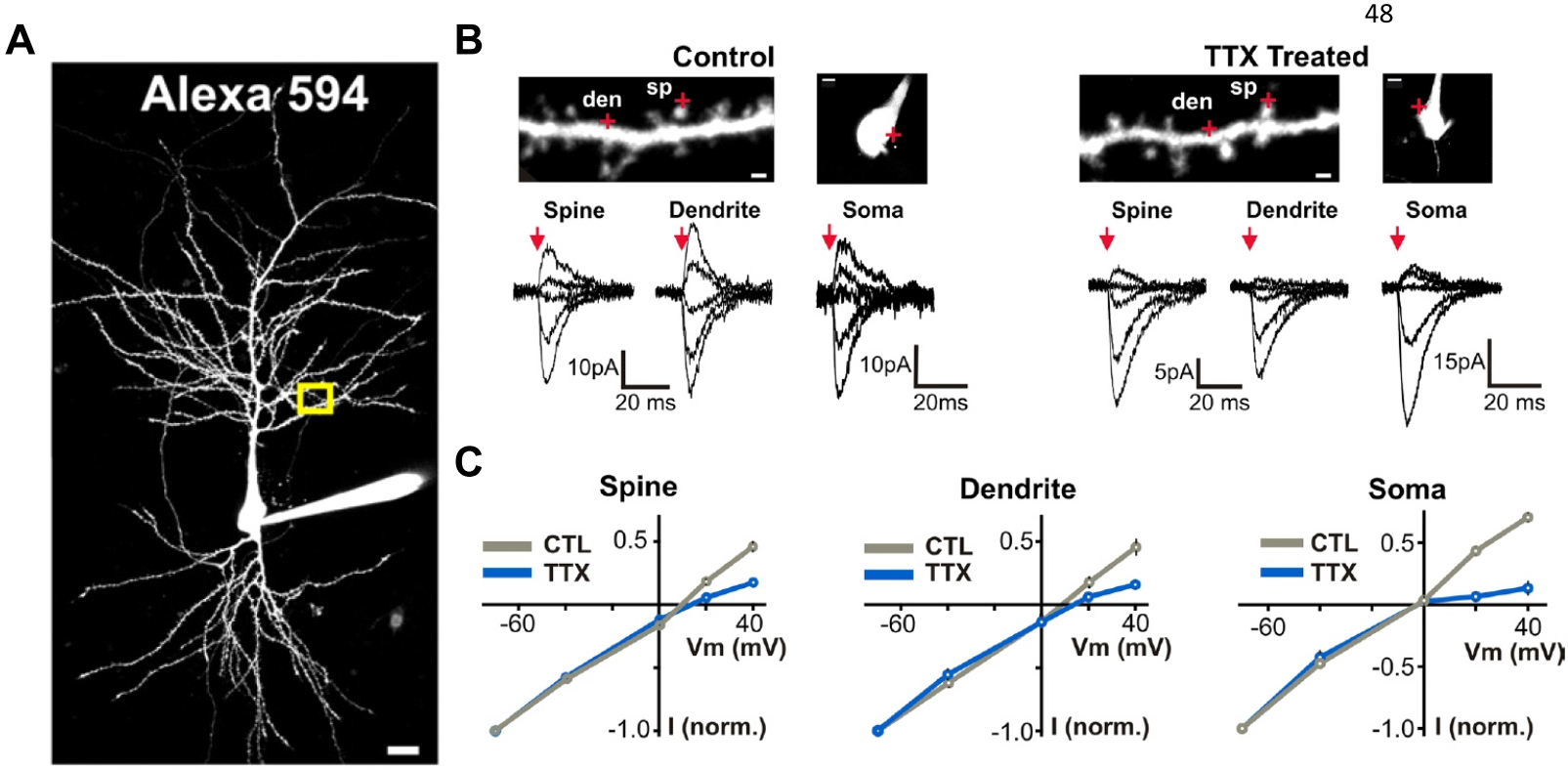

Figure 5. Cell-wide upregulation of GluA2-lacking AMPARs in response to prolonged TTX treatment (72 hours). **A**, 2P image of a CA1 pyramidal neuron filled with Alexa Fluor 594 to visualize dendritic morphology. **B**, I–V relationship of AMPAR-2P -EPSCs generated at distinct subcellular locations. 2P images of soma and secondary apical dendritic segments show sites of glutamate uncaging (red crosshairs), and AMPAR-2P-EPSCs at different holding potentials (-60 to -40 mV; with 100 μM intracellular spermine). **C**, Average I–V curves of 2P-EPSCs from each subcellular location in both control and TTX conditions (Soares *et al.*, 2013).

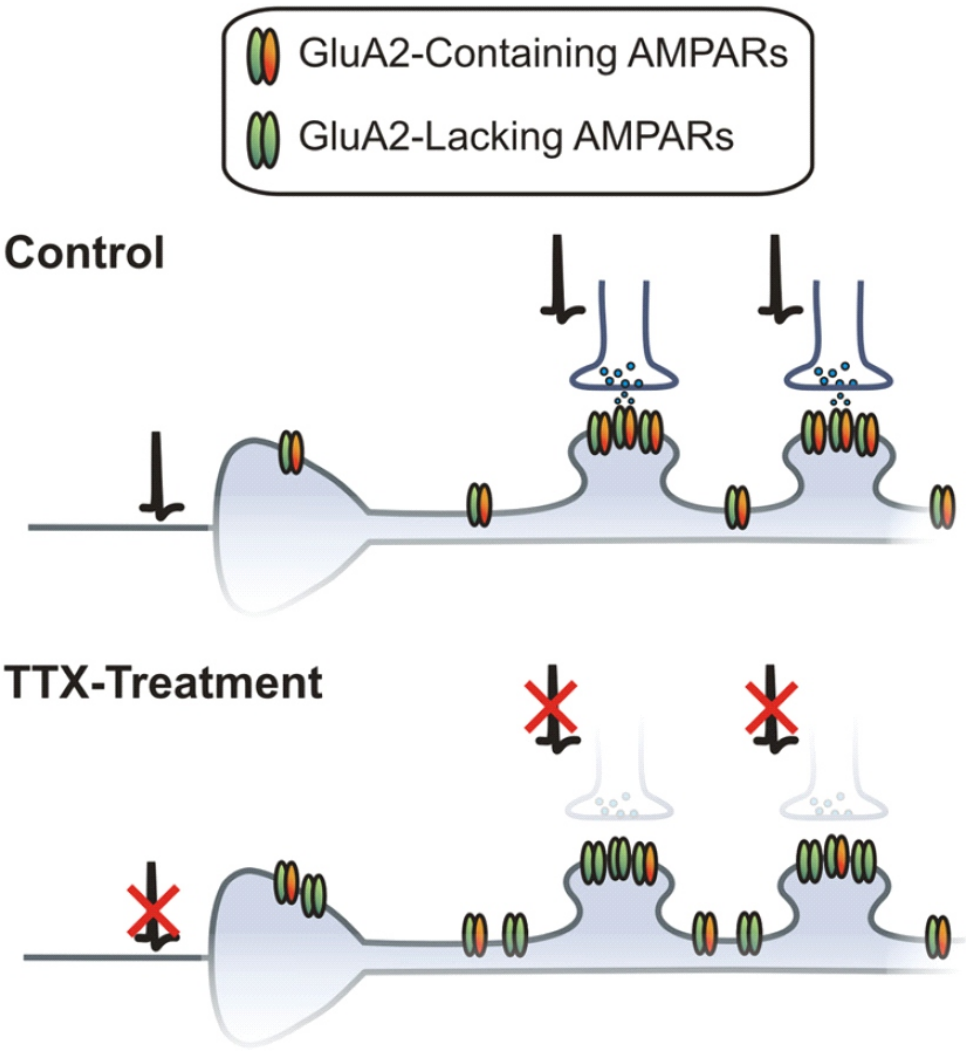

Figure 6. Homeostatic Synaptic Plasticity (HSP) model for AMPA receptors. In control conditions, the AMPA receptor population is largely comprised of GluA2-containing AMPA receptors. After prolonged activity deprivation (TTX treatment), AMPA receptors undergo a subunit switch from GluA2-containing (calcium-impermeable) to GluA2-lacking (calcium-permeable) (Soares *et al.*, 2013).

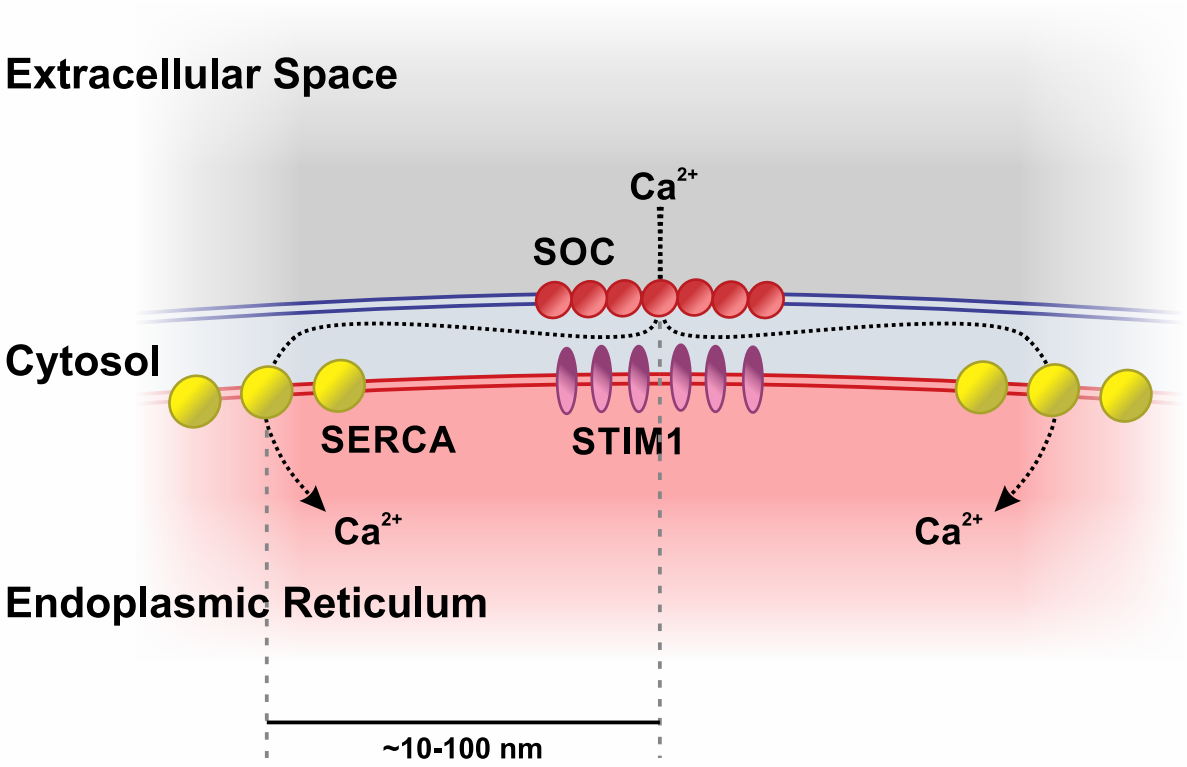

Figure 7. Store-operated responses in the endoplasmic reticulum (ER). A transverse ER membrane Ca^{2+} sensor – Stromal interaction molecule (STIM1) – senses the depletion of Ca^{2+} with its N-terminal tail (Roos *et al.*, 2005). STIM1 then aggregates and migrates to the ER-plasma membrane junction and activates Ca^{2+} channels at the plasma membrane (Luik *et al.*, 2006). Channels that areactivated by the depletion of $[Ca^{2+}]_{ER}$ are referred to as store-operated Ca^{2+} channels (SOC). Calcium then rushes back into the ER through sarco/endoplasmic reticulum Ca^{2+} ATPases (SERCA).

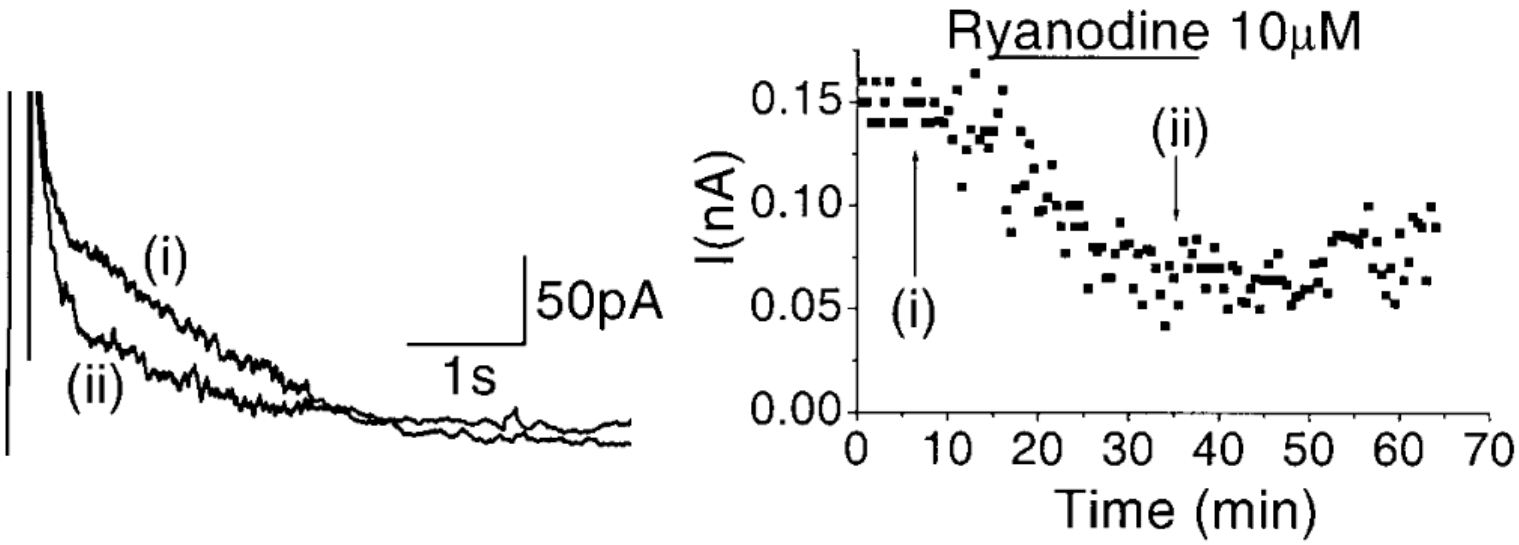

Figure 8. The slow AHP in CA1 pyramidal neurons is reduced by more than 50% with application of 10 μM ryanodine, a ryanodine receptor antagonist (Shah & Haylett, 2000).

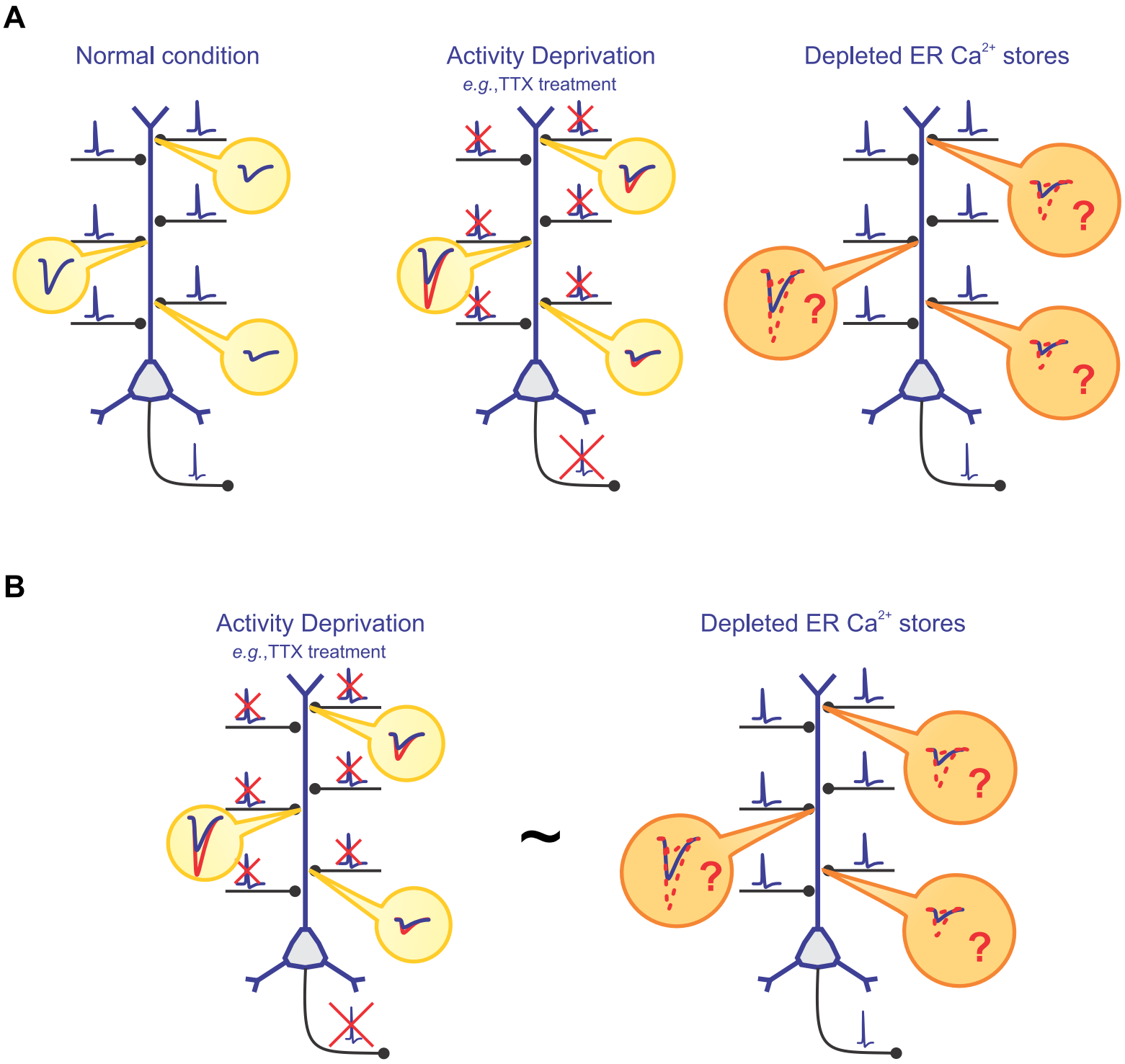

Figure 9. Main Objectives. **A**, To determine whether the regulation of a population of glutamate receptor subunits is part of the store-operated response in central neurons. **B**, To determine whether homeostatic synaptic plasticity is a store operated response.

Results Figures

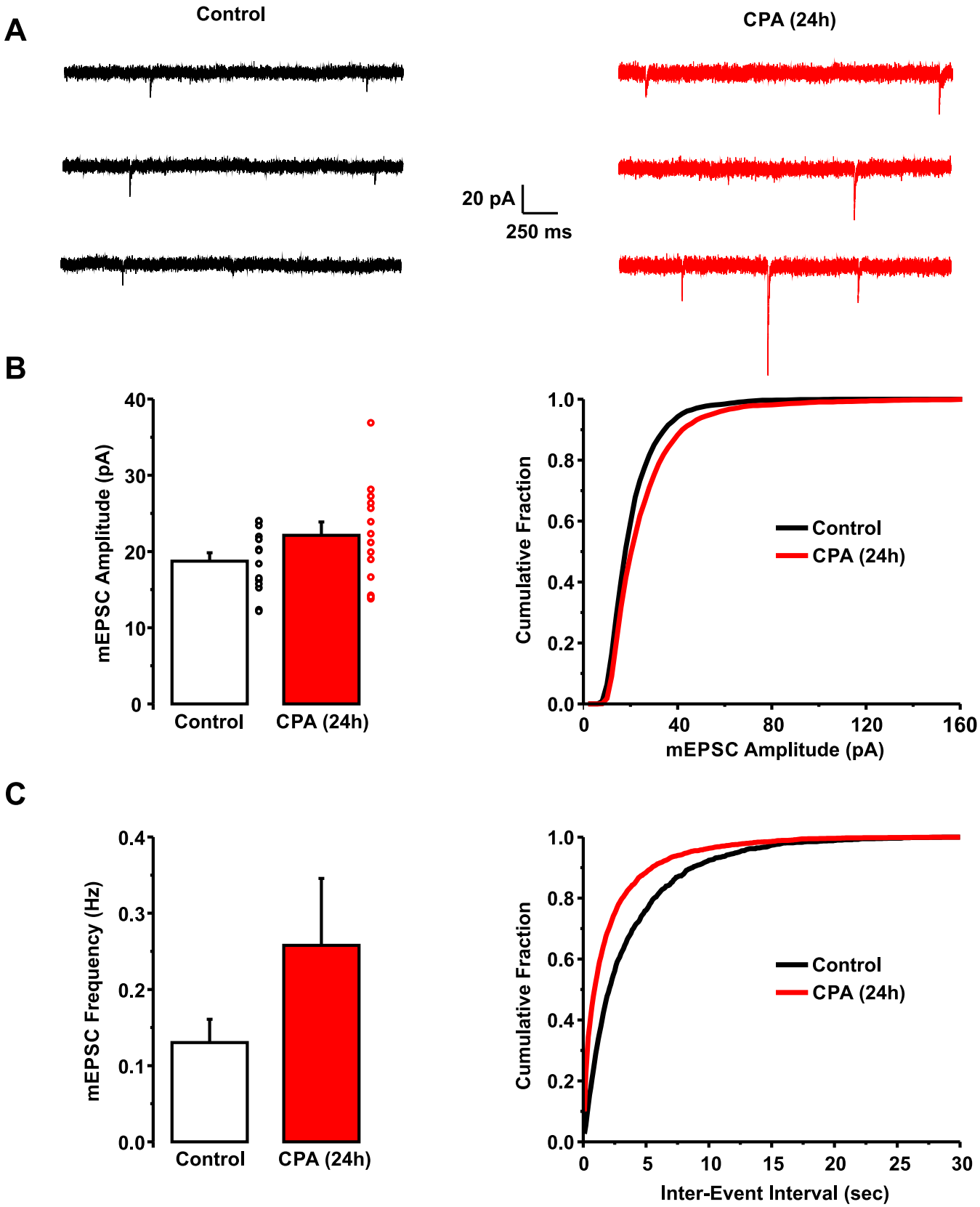

Figure 10. Potentiation of CA1 pyramidal neurons after 24 hour CPA treatment. **A**, Sample current traces of AMPAR-mediated miniature EPSCs in control and CPA treated hippocampal CA1 pyramidal neurons recorded at -70 mV voltage clamp. **B**, Average AMPAR-mediated miniature EPSC amplitudes (left) (p-value = 0.115; unpaired Student's t test) and a cumulative distribution of all AMPAR-mediated miniature EPSC amplitudes (right) (p-value < 0.001; ks test). **C**, Average AMPAR-mediated miniature EPSC frequencies (left) (p-value = 0.189; unpaired Student's t test) and a cumulative distribution of the interval between miniature EPSCs (right) (p-value < 0.001; ks test). Error bars represent standard error of the mean (n = 14 for control; n = 14 for CPA).

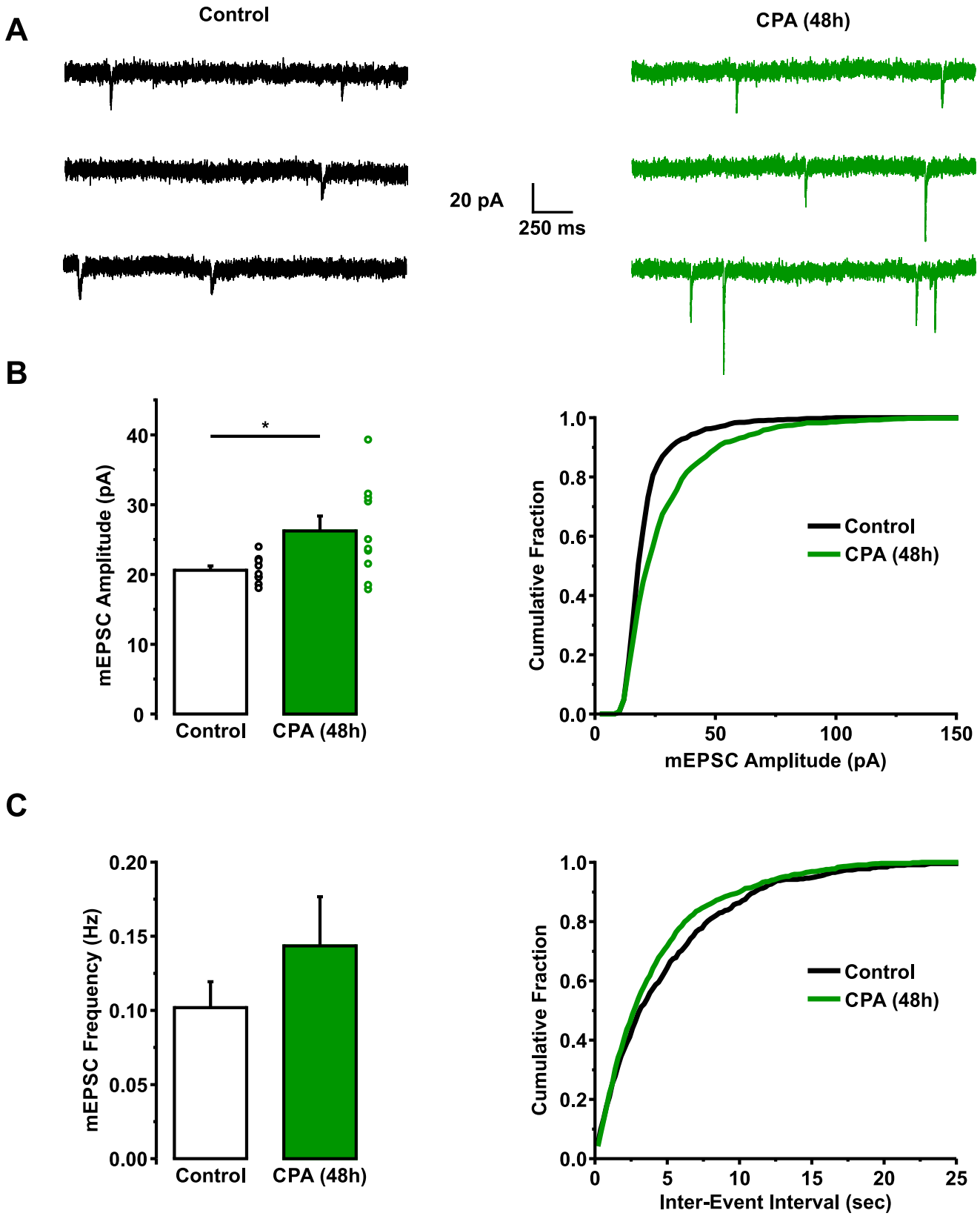

Figure 11. Potentiation of CA1 pyramidal neurons after 48 hour CPA treatment. **A**, Sample current traces of AMPAR-mediated miniature EPSCs in control and CPA treated hippocampal CA1 pyramidal neurons recorded at -70 mV voltage clamp. **B**, Average AMPAR-mediated miniature EPSC amplitudes (left) (p-value < 0.05; unpaired Student's t test) and a cumulative distribution of all AMPAR-mediated miniature EPSC amplitudes (right) (p-value < 0.001; ks test). **C**, Average AMPAR-mediated miniature EPSC frequencies (left) (p-value = 0.286; unpaired Student's t test) and a cumulative distribution of the interval between miniature EPSCs (right) (p-value < 0.001; ks test). Error bars represent standard error of the mean (n = 9 for control; n = 10 for CPA).

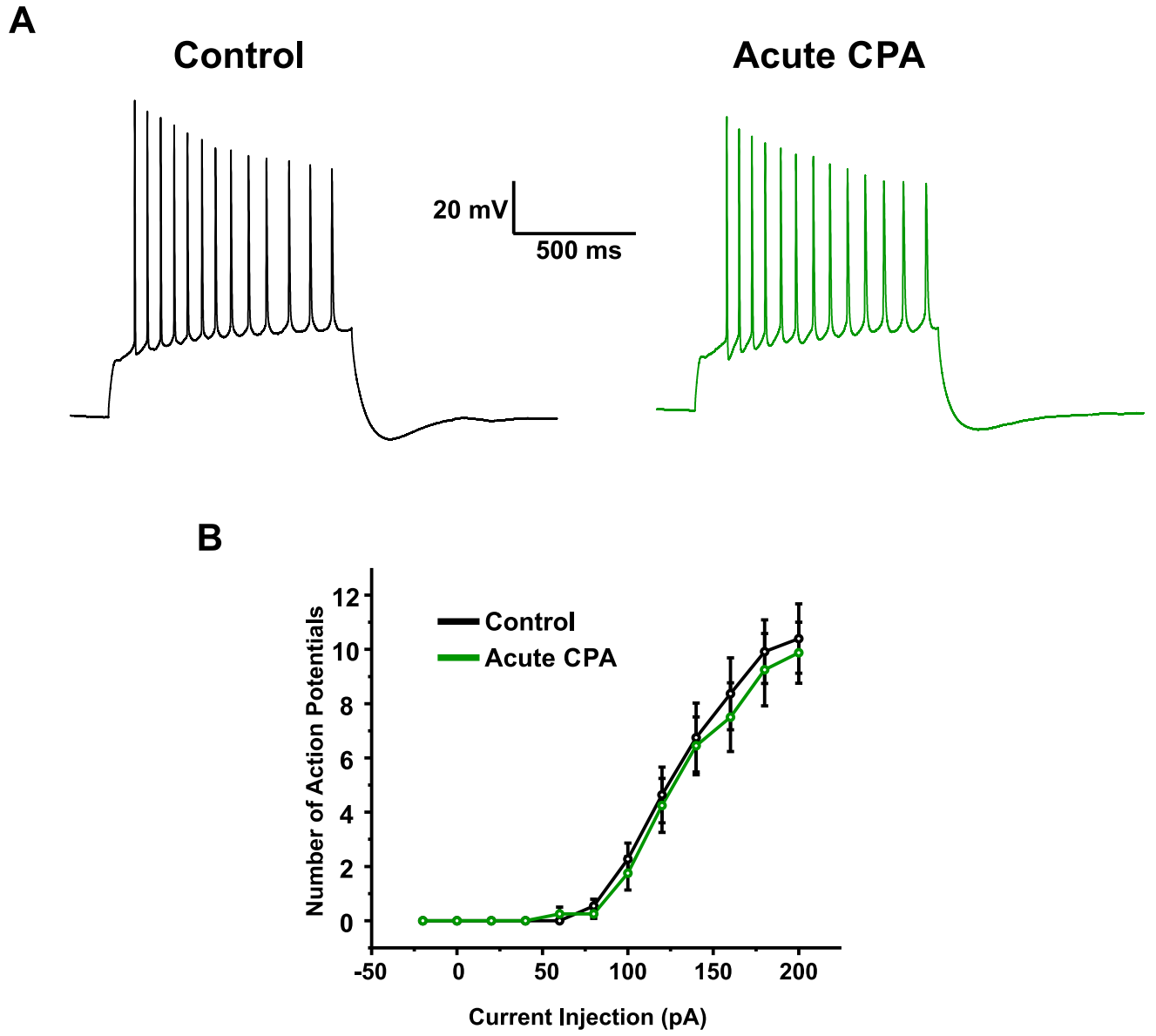

Figure 12. Acute CPA treatment has no effect on firing rate. **A**, Sample traces of action potential firing in control and CPA treated hippocampal CA1 pyramidal neurons during a 200 pA step recorded in current clamp. **B**, Number of action potentials fired versus the amount of current injected. Error bars represent standard error of the mean (n = 12 for control; n = 9 for CPA).

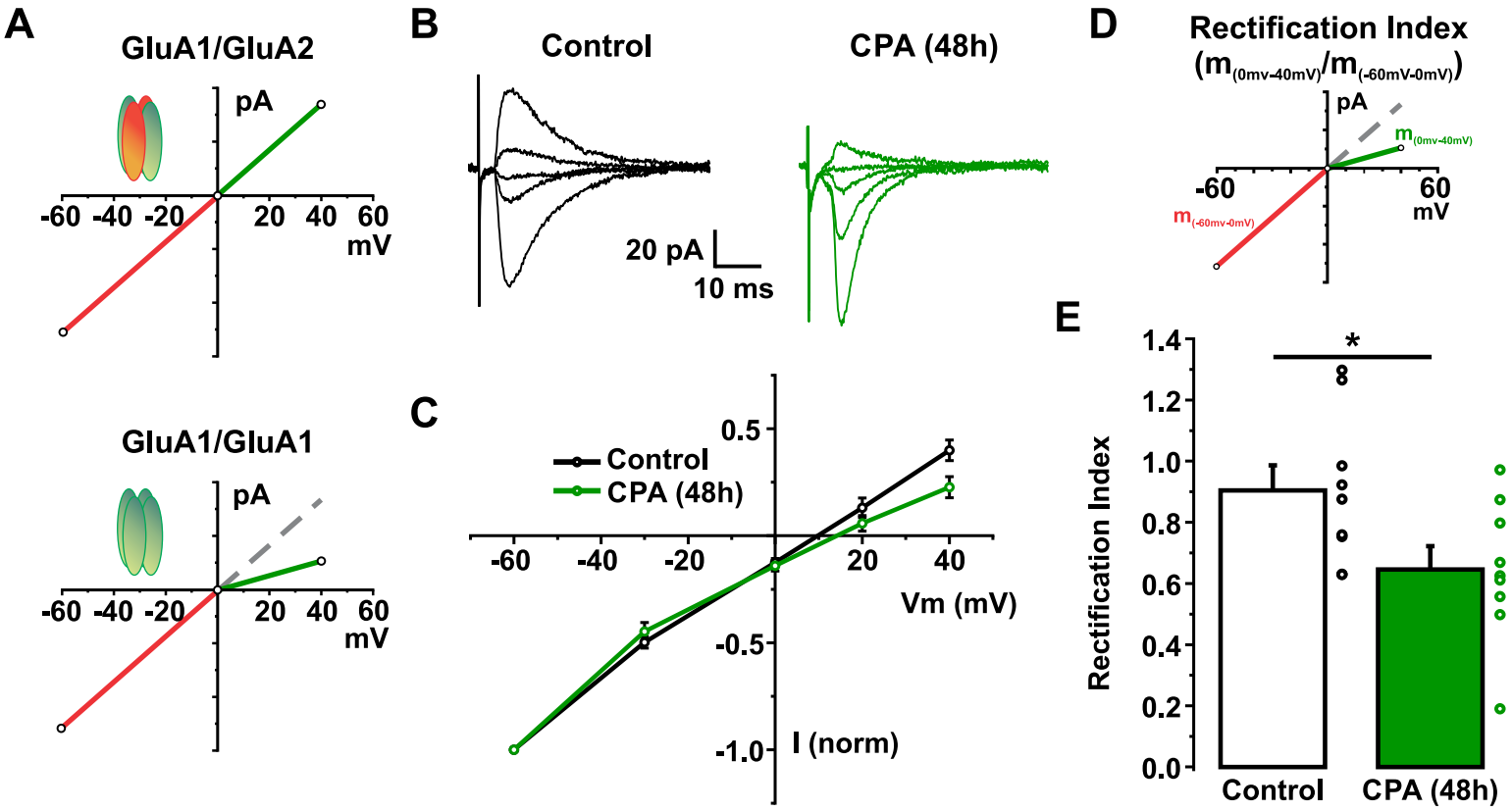

Figure 13. Insertion of GluA2-lacking AMPARs after 48 hour CPA treatment. **A**, I–V relationship of evoked AMPAR-EPSCs. **B**, Current traces at different holding potentials (-60 to -40 mV; with 100 μM intracellular spermine). **C**, Average I-V curves of evoked AMPAR-mediated EPSCs from control and CPA treated neurons. These currents were generated by stimulating CA3 pyramidal neuron, which synapse onto CA1 neurons. **D**, Rectification index is the ratio of the I-V slope of the outward current over the I-V slope of the inward current. **E**, Average AMPAR Rectification Indices ($p < 0.05$; unpaired Student's t test; n = 9 for control; n = 10 for CPA). Error bars in bar graphs represent standard error of the mean.

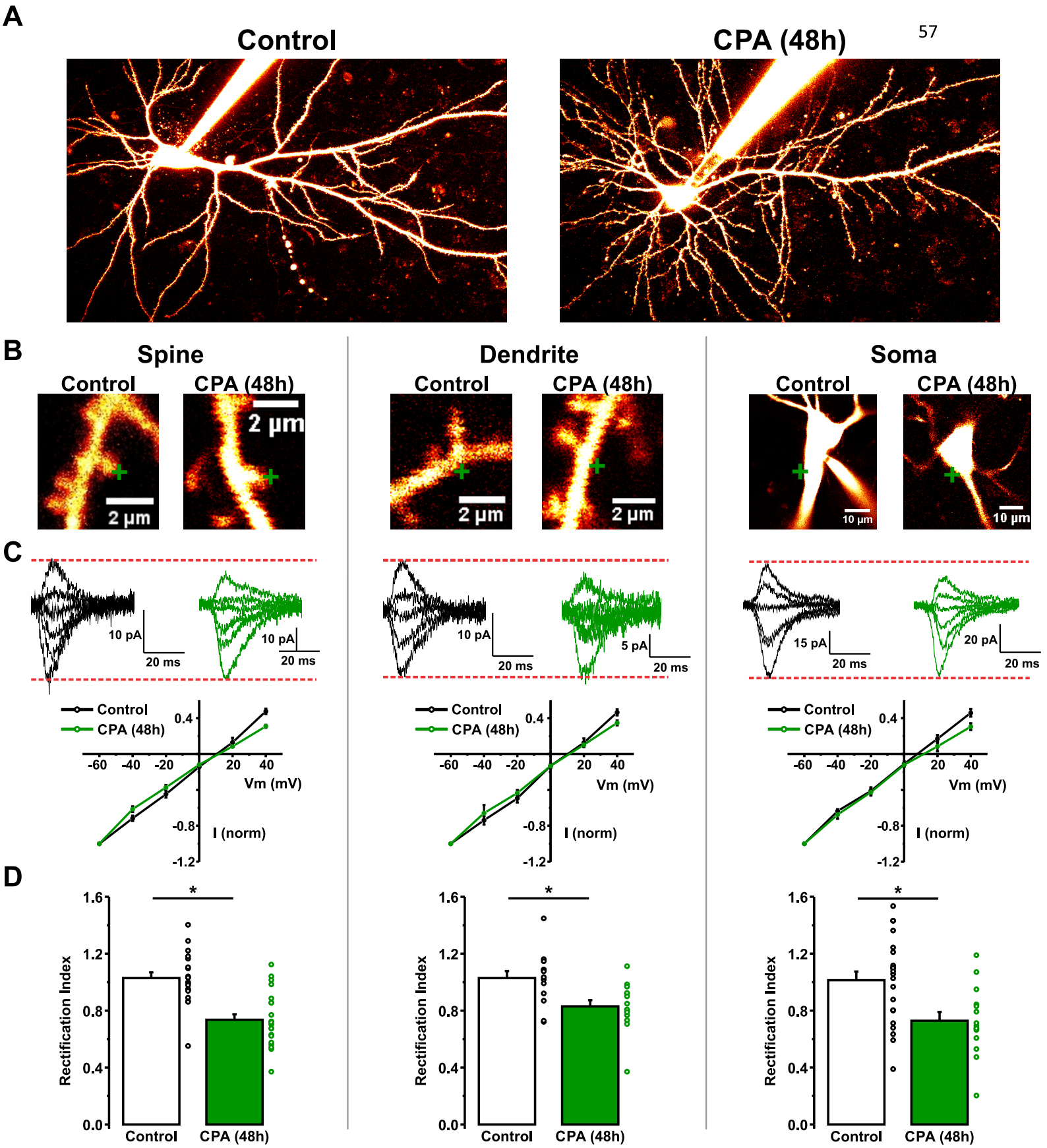

Figure 14. Cell-wide upregulation of GluA2-lacking AMPARs in response to 48 hour CPA treatment. **A**, 2P image of a control and CPA CA1 pyramidal neuron filled with Alexa Fluor 594 to visualize dendritic morphology. **B**, I–V relationship of AMPAR-2P-EPSCs generated at distinct subcellular locations. 2P images of soma and secondary apical dendritic segments show sites of glutamate uncaging (gray crosshairs). **C**, AMPAR-2P-EPSCs at different holding potentials (-60 to -40 mV; with 100 µM intracellular spermine). Average I–V curves of 2P-EPSCs from each subcellular location in both control and CPA conditions. **D**, Rectification indices for all spine, dendritic, and somatic I–V curves presented in **C** ($p < 0.01$; unpaired Student's t test; n = 20 for control spine; n = 23 for CPA spine; n = 14 for control dendrite; n = 15 for CPA dendrite; n = 23 for control soma; n = 15 for CPA soma). Error bars represent standard error of the mean.

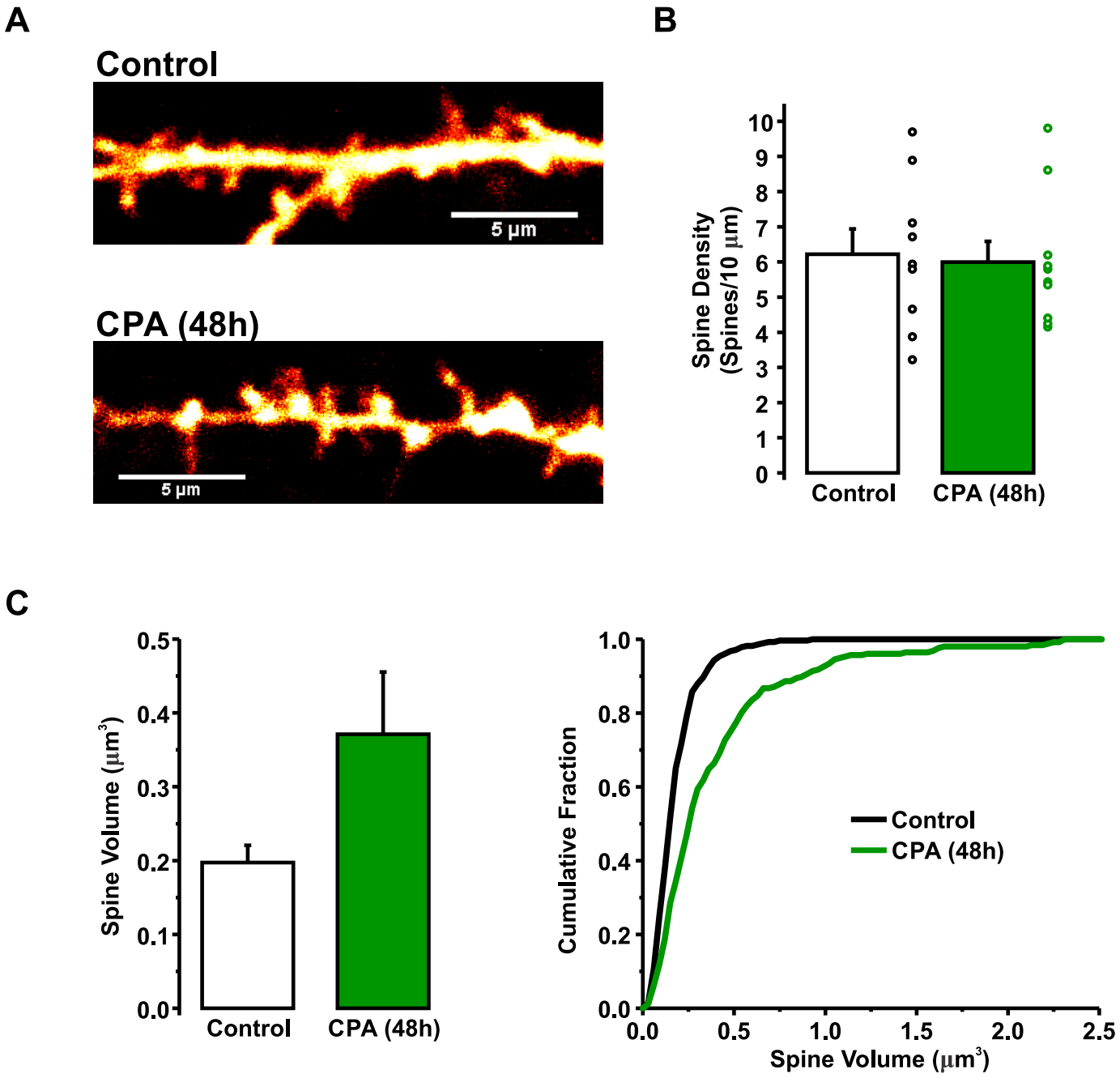

Figure 15. Spine density and spine volume of control and 48 hour CPA-treated CA1 pyramidal neurons. **A**, Two-photon image stacks of CA1 pyramidal apical dendrites filled with Alexa Fluor 594. **B**, Average density of dendritic spines on apical dendrites of filled CA1 pyramidal neurons (p-value = 0.814; unpaired Student's t test; n = 9 for control; n = 10 for CPA). **C**, Average spine volume on apical dendrites of filled CA1 pyramidal neurons (left) (p-value = 0.0968; unpaired Student's t test; n = 5 for control; n = 6 for CPA) and a cumulative distribution of all spine volumes (right) (p-value < 0.001; ks test). Error bars represent standard error of the mean.

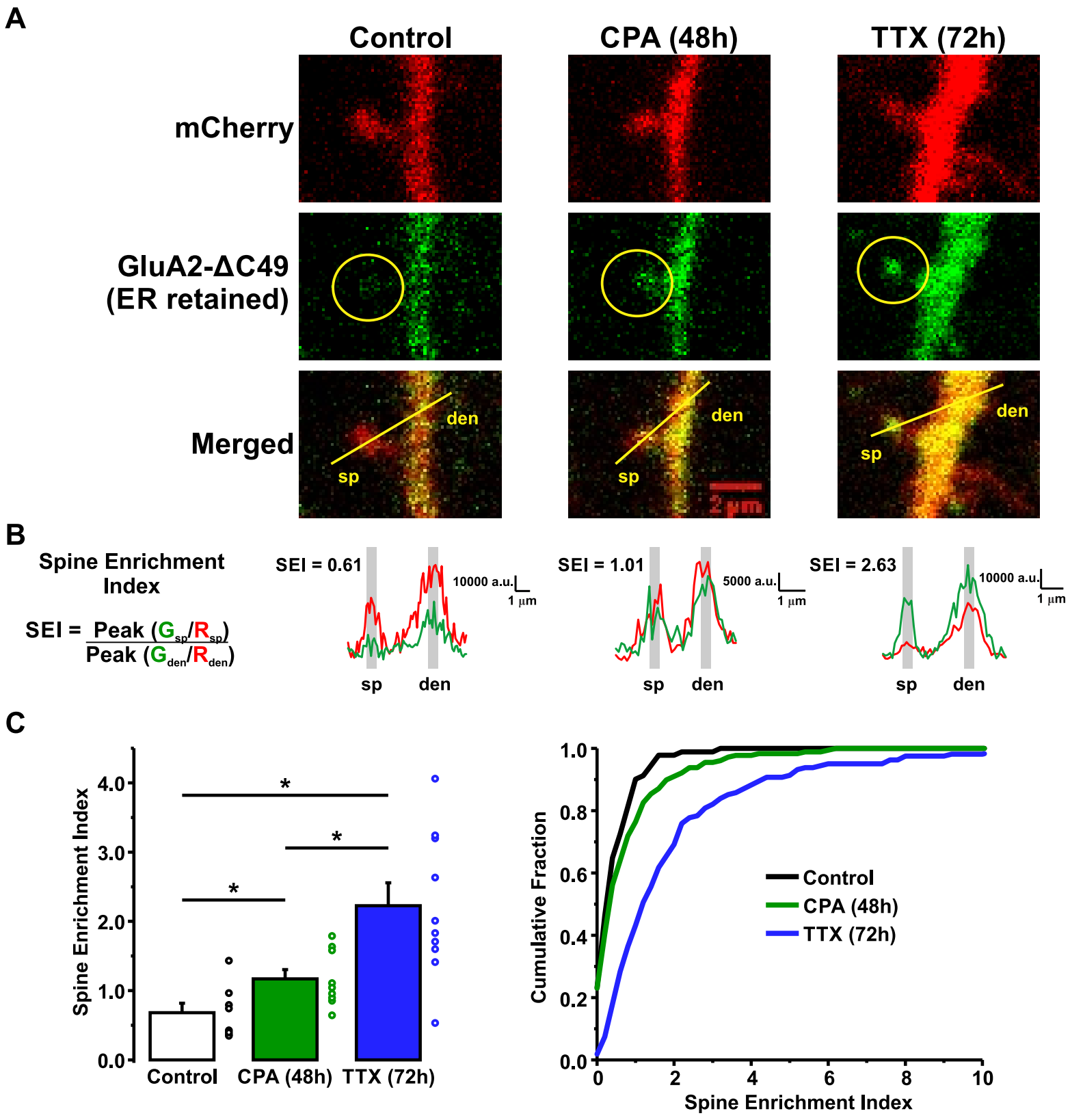

Figure 16. The Endoplasmic Reticulum (ER) invades spines after prolonged CPA and TTX treatment. **A**, Two-photon image stacks of CA1 pyramidal apical dendrites biolistically transfected with mCherry and pHluorin-GluA2 ΔC49 (ER-retained protein). **B**, Spine Enrichment Index equation and sample spines and sample line ROI curves. **C**, Average spine enrichment index (left) (p-value < 0.05; One-way ANOVA with post-hoc Tukey HSD test; n = 8 control; n = 9 for CPA; n = 10 for TTX) and a cumulative distribution of all spine enrichment indices (right) (CPA vs Control, p-value < 0.001, ks test; TTX vs Control, p-value < 0.001, ks test; TTX vs CPA, p-value < 0.001, ks test). Error bars represent standard error of the mean.

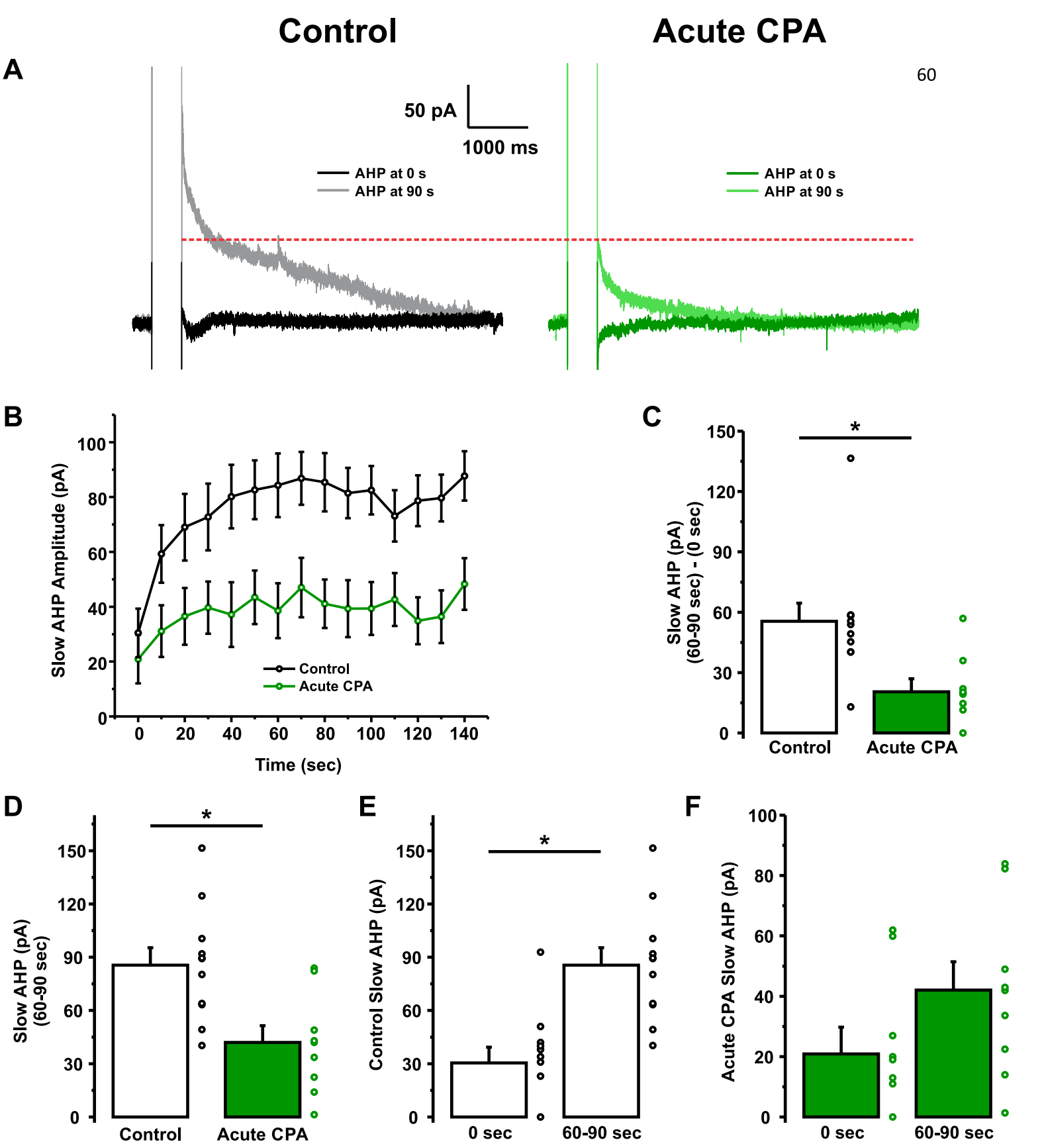

Figure 17. The slow AHP in CA1 pyramidal neurons is partially blocked by acute CPA treatment. **A**, Sample traces of AHP in voltage clamp at different time points. **B**, Time course of the slow AHP amplitude. **C**, Average of the difference between the slow AHP at 0 seconds and the slow AHP at 60-90 seconds (p-value < 0.01; unpaired Student's t test; n = 11 for control; n = 9 for acute CPA). **D**, Average slow AHP at 60-90 seconds (p-value < 0.01; unpaired Student's t test; n = 11 for control; n = 9 for acute CPA). **E**, Average slow AHP at 0 seconds and 60-90 seconds for control cells (p-value < 0.01; paired Student's t test; n = 11 for control at 0 seconds; n = 11 for control at 60-90 seconds). **F**, Average slow AHP at 0 seconds and 60-90 seconds for acute CPA treated cells (p-value = 0.133; paired Student's t test; n = 9 for acute CPA at 0 seconds; n = 9 for acute CPA at 60-90 seconds). Error bars represent standard error of the mean.

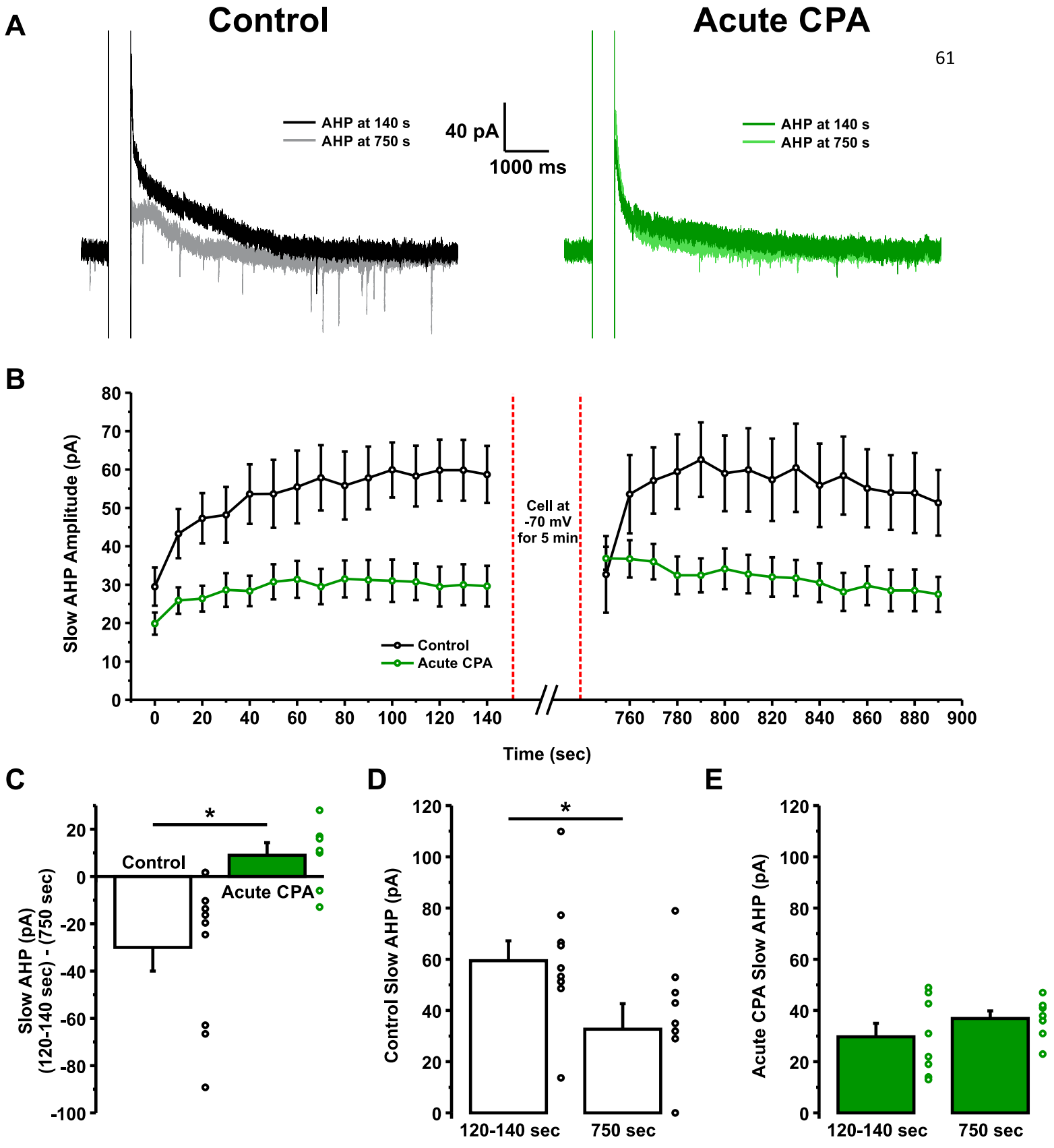

Figure 18. The decrease of the slow AHP in CA1 pyramidal neurons during resting membrane potential is blocked by acute CPA treatment. **A**, Sample traces of AHP in voltage clamp at different time points. **B**, Time course of the slow AHP amplitude. **C**, Average of the difference between the slow AHP at 120-140 seconds and the slow AHP at 750 seconds (p-value < 0.01; unpaired Student's t test; n = 10 for control; n = 8 for acute CPA). **D**, Average slow AHP at 120-140 seconds and 750 seconds for control cells (p-value < 0.05; paired Student's t test; n = 10 for control at 120-140 seconds; n = 10 for control at 750 seconds). **E**, Average slow AHP at 120-140 seconds and 750 seconds for acute CPA treated cells (p-value = 0.276; paired Student's t test; n = 8 for acute CPA at 120-140 seconds; n = 8 for acute CPA at 750 seconds). Error bars represent standard error of the mean.

Discussion Figure

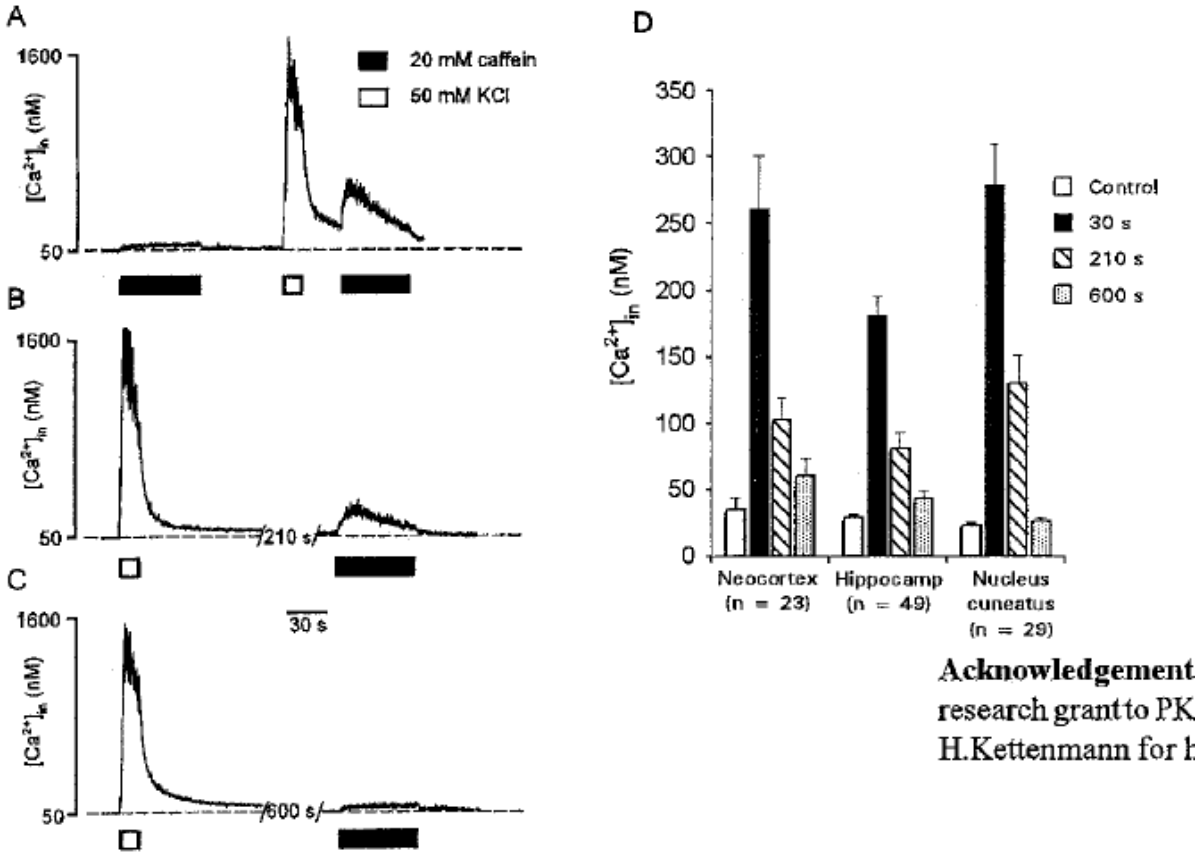

Figure 19. ER calcium is low in central neurons under resting membrane potential. Under resting membrane potential, central neurons (including CA1 pyramidal neurons) have a very low level of ER calcium, and this is only replenished by depolarizing the cell to open voltage-gated calcium channels (in this case, the cell is depolarised with 50 mM Kcl and calcium is released with 20 mM caffein) (Shmigol *et al.*, 1994).

Conclusion Figure

A. Normal Conditions

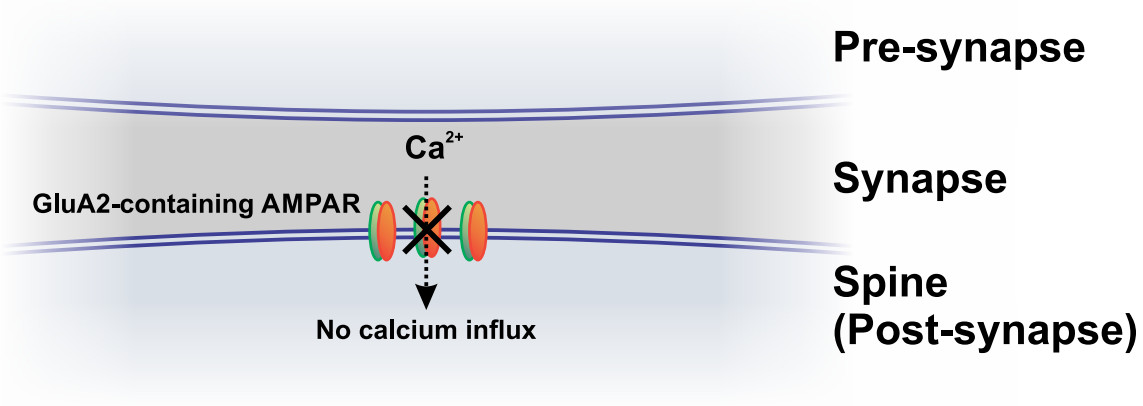

B. Activity Deprivation or Depleted ER Ca^{2+} stores

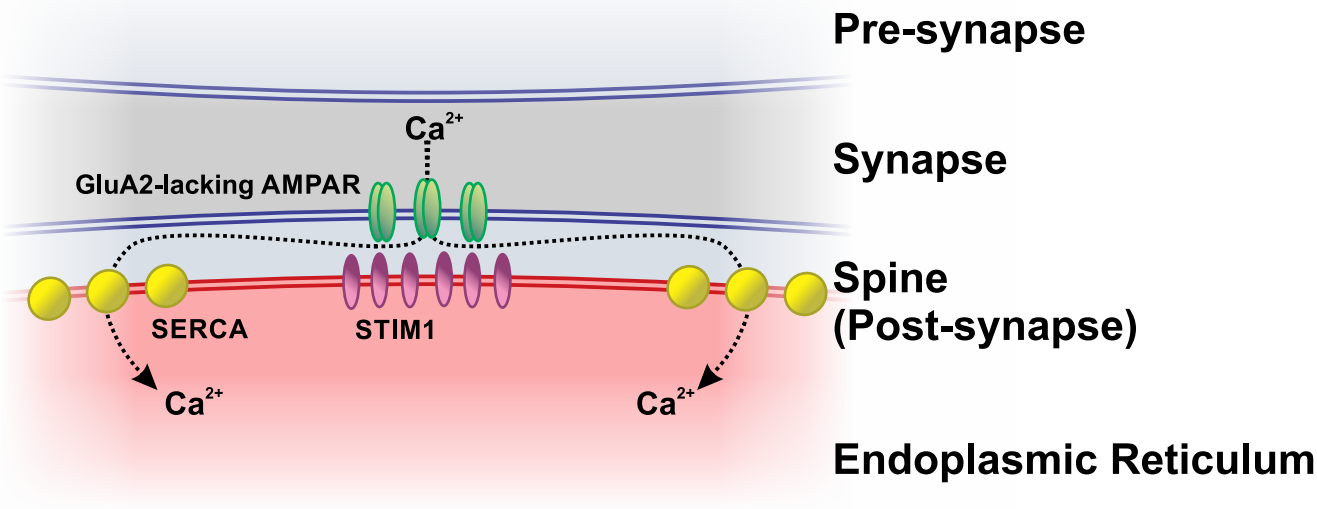

Figure 20. Model supported by the data. A, Under normal conditions, CA1 pyramidal neurons express GluA2-containing AMPA receptors, with very few spines invaded by ER. B, After prolonged activity deprivation or depleted ER Ca^{2+} stores, a subunit shift from GluA2-containing to GluA2-lacking AMPA receptors occurs, and a larger number of spines is invaded by ER. This may be a compensatory mechanism to refill depleted ER Ca^{2+} stores which would bring a significant paradigm shift in our understanding of HSP and the store-operated response in central neurons.

NATURE PUBLISHING GROUP LICENSE TERMS AND CONDITIONS

Nov 06, 2015

This is a License Agreement between Wissam Nassrallah ("You") and Nature Publishing Group ("Nature Publishing Group") provided by Copyright Clearance Center ("CCC"). The license consists of your order details, the terms and conditions provided by Nature Publishing Group, and the payment terms and conditions.

All payments must be made in full to CCC. For payment instructions, please see information listed at the bottom of this form.

License Number	3743380125499
License date	Nov 06, 2015
Licensed content publisher	Nature Publishing Group
Licensed content publication	Nature Reviews Neuroscience
Licensed content title	Homeostatic plasticity in the developing nervous system
Licensed content author	Gina G. TurrigianoandSacha B. Nelson
Licensed content date	Feb 1, 2004
Volume number	5
Issue number	2
Type of Use	reuse in a dissertation / thesis
Requestor type	academic/educational
Format	electronic
Portion	figures/tables/illustrations
Number of figures/tables /illustrations	1
High-res required	no
Figures	Figure 2
Author of this NPG article	no
Your reference number	None
Title of your thesis / dissertation	Store-Operated Response in CA1 Pyramidal Neurons Exhibits Features of Homeostatic Synaptic Plasticity
Expected completion date	Nov 2015
Estimated size (number of pages)	80
Total	0.00 CAD
Terms and Conditions	

Terms and Conditions for Permissions

Nature Publishing Group hereby grants you a non-exclusive license to reproduce this material for this purpose, and for no other use,subject to the conditions below:

1. NPG warrants that it has, to the best of its knowledge, the rights to license reuse of this material. However, you should ensure that the material you are requesting is original to Nature Publishing Group and does not carry the copyright of another entity (as credited in the published version). If the credit line on any part of the material you have requested indicates that it was reprinted or adapted by NPG with permission from another source, then you should also seek permission from that source to reuse the material.

2. Permission granted free of charge for material in print is also usually granted for any electronic version of that work, provided that the material is incidental to the work as a whole and that the electronic version is essentially equivalent to, or substitutes for, the print version.Where print permission has been granted for a fee, separate permission must be obtained for any additional, electronic re-use (unless, as in the case of a full paper, this has already been accounted for during your initial request in the calculation of a print run).NB: In all cases, web-based use of full-text articles must be authorized separately through the 'Use on a Web Site' option when requesting permission.

3. Permission granted for a first edition does not apply to second and subsequent editions and for editions in other languages (except for signatories to the STM Permissions Guidelines, or where the first edition permission was granted for free).

4. Nature Publishing Group's permission must be acknowledged next to the figure, table or abstract in print. In electronic form, this acknowledgement must be visible at the same time as the figure/table/abstract, and must be hyperlinked to the journal's homepage.

5. The credit line should read:
   Reprinted by permission from Macmillan Publishers Ltd: [JOURNAL NAME] (reference citation), copyright (year of publication) For AOP papers, the credit line should read:
   Reprinted by permission from Macmillan Publishers Ltd: [JOURNAL NAME], advance online publication, day month year (doi: 10.1038/sj.[JOURNAL ACRONYM].XXXXX)

   Note: For republication from the *British Journal of Cancer,* the following credit lines apply.
   Reprinted by permission from Macmillan Publishers Ltd on behalf of Cancer Research UK: [JOURNAL NAME] (reference citation), copyright (year of publication)For AOP papers, the credit line should read:
   Reprinted by permission from Macmillan Publishers Ltd on behalf of Cancer Research UK: [JOURNAL NAME], advance online publication, day month year (doi: 10.1038/sj.[JOURNAL ACRONYM].XXXXX)

6. Adaptations of single figures do not require NPG approval. However, the adaptation should be credited as follows:

   Adapted by permission from Macmillan Publishers Ltd: [JOURNAL NAME] (reference citation), copyright (year of publication)

   Note: For adaptation from the *British Journal of Cancer,* the following credit line applies.
   Adapted by permission from Macmillan Publishers Ltd on behalf of Cancer Research UK: [JOURNAL NAME] (reference citation), copyright (year of publication)

7. Translations of 401 words up to a whole article require NPG approval. Please visit http://www.macmillanmedicalcommunications.com for more information.Translations of up to a 400 words do not require NPG approval. The translation should be credited as follows:

   Translated by permission from Macmillan Publishers Ltd: [JOURNAL NAME] (reference citation), copyright (year of publication).

   Note: For translation from the *British Journal of Cancer,* the following credit line applies.
   Translated by permission from Macmillan Publishers Ltd on behalf of Cancer Research UK: [JOURNAL NAME] (reference citation), copyright (year of publication)

We are certain that all parties will benefit from this agreement and wish you the best in the use of this material. Thank you.

Special Terms:
v1.1

NATURE PUBLISHING GROUP LICENSE TERMS AND CONDITIONS

Nov 06, 2015

This is a License Agreement between Wissam Nassrallah ("You") and Nature Publishing Group ("Nature Publishing Group") provided by Copyright Clearance Center ("CCC"). The license consists of your order details, the terms and conditions provided by Nature Publishing Group, and the payment terms and conditions.

All payments must be made in full to CCC. For payment instructions, please see information listed at the bottom of this form.

License Number	3743381125420
License date	Nov 06, 2015
Licensed content publisher	Nature Publishing Group
Licensed content publication	Nature
Licensed content title	Activity-dependent scaling of quantal amplitude in neocortical neurons
Licensed content author	Gina G. Turrigiano, Kenneth R. Leslie, Niraj S. Desai, Lana C. Rutherford and Sacha B. Nelson
Licensed content date	Feb 26, 1998
Volume number	391
Issue number	6670
Type of Use	reuse in a dissertation / thesis
Requestor type	academic/educational
Format	electronic
Portion	figures/tables/illustrations
Number of figures/tables /illustrations	1
Figures	Figure 1
Author of this NPG article	no
Your reference number	None
Title of your thesis / dissertation	Store-Operated Response in CA1 Pyramidal Neurons Exhibits Features of Homeostatic Synaptic Plasticity
Expected completion date	Nov 2015
Estimated size (number of pages)	80
Total	0.00 CAD
Terms and Conditions	

Terms and Conditions for Permissions

Nature Publishing Group hereby grants you a non-exclusive license to reproduce this material for this purpose, and for no other use,subject to the conditions below:

1. NPG warrants that it has, to the best of its knowledge, the rights to license reuse of this material. However, you should ensure that the material you are requesting is original to Nature Publishing Group and does not carry the copyright of another entity (as credited in the published version). If the credit line on any part of the material you have requested

indicates that it was reprinted or adapted by NPG with permission from another source, then you should also seek permission from that source to reuse the material.

2. Permission granted free of charge for material in print is also usually granted for any electronic version of that work, provided that the material is incidental to the work as a whole and that the electronic version is essentially equivalent to, or substitutes for, the print version.Where print permission has been granted for a fee, separate permission must be obtained for any additional, electronic re-use (unless, as in the case of a full paper, this has already been accounted for during your initial request in the calculation of a print run).NB: In all cases, web-based use of full-text articles must be authorized separately through the 'Use on a Web Site' option when requesting permission.

3. Permission granted for a first edition does not apply to second and subsequent editions and for editions in other languages (except for signatories to the STM Permissions Guidelines, or where the first edition permission was granted for free).

4. Nature Publishing Group's permission must be acknowledged next to the figure, table or abstract in print. In electronic form, this acknowledgement must be visible at the same time as the figure/table/abstract, and must be hyperlinked to the journal's homepage.

5. The credit line should read:
   Reprinted by permission from Macmillan Publishers Ltd: [JOURNAL NAME] (reference citation), copyright (year of publication) For AOP papers, the credit line should read:
   Reprinted by permission from Macmillan Publishers Ltd: [JOURNAL NAME], advance online publication, day month year (doi: 10.1038/sj.[JOURNAL ACRONYM].XXXXX)

   Note: For republication from the *British Journal of Cancer,* the following credit lines apply.
   Reprinted by permission from Macmillan Publishers Ltd on behalf of Cancer Research UK: [JOURNAL NAME] (reference citation), copyright (year of publication)For AOP papers, the credit line should read:
   Reprinted by permission from Macmillan Publishers Ltd on behalf of Cancer Research UK: [JOURNAL NAME], advance online publication, day month year (doi: 10.1038/sj.[JOURNAL ACRONYM].XXXXX)

6. Adaptations of single figures do not require NPG approval. However, the adaptation should be credited as follows:

   Adapted by permission from Macmillan Publishers Ltd: [JOURNAL NAME] (reference citation), copyright (year of publication)

   Note: For adaptation from the *British Journal of Cancer,* the following credit line applies.
   Adapted by permission from Macmillan Publishers Ltd on behalf of Cancer Research UK: [JOURNAL NAME] (reference citation), copyright (year of publication)

7. Translations of 401 words up to a whole article require NPG approval. Please visit http://www.macmillanmedicalcommunications.com for more information.Translations of up to a 400 words do not require NPG approval. The translation should be credited as follows:

   Translated by permission from Macmillan Publishers Ltd: [JOURNAL NAME] (reference citation), copyright (year of publication).

   Note: For translation from the *British Journal of Cancer,* the following credit line applies.
   Translated by permission from Macmillan Publishers Ltd on behalf of Cancer Research UK: [JOURNAL NAME] (reference citation), copyright (year of publication)

We are certain that all parties will benefit from this agreement and wish you the best in the use of this material. Thank you.

Special Terms:
v1.1

Questions? customercare@copyright.com or +1-855-239-3415 (toll free in the US) or +1-978-646-2777.

SPRINGER LICENSE TERMS AND CONDITIONS

Nov 06, 2015

This is a License Agreement between Wissam Nassrallah ("You") and Springer ("Springer") provided by Copyright Clearance Center ("CCC"). The license consists of your order details, the terms and conditions provided by Springer, and the payment terms and conditions.

All payments must be made in full to CCC. For payment instructions, please see information listed at the bottom of this form.

License Number	3743390231815
License date	Nov 06, 2015
Licensed content publisher	Springer
Licensed content publication	Pflügers Archiv European Journal of Physiology
Licensed content title	Different properties of caffeine-sensitive Ca2+ stores in peripheral and central mammalian neurones
Licensed content author	Anatoly Shmigol
Licensed content date	Jan 1, 1994
Volume number	426
Issue number	1
Type of Use	Thesis/Dissertation
Portion	Figures/tables/illustrations
Number of figures/tables /illustrations	1
Author of this Springer article	No
Order reference number	None
Original figure numbers	Figure 2
Title of your thesis / dissertation	Store-Operated Response in CA1 Pyramidal Neurons Exhibits Features of Homeostatic Synaptic Plasticity
Expected completion date	Nov 2015
Estimated size(pages)	80
Total	0.00 CAD
Terms and Conditions	

Introduction

The publisher for this copyrighted material is Springer Science + Business Media. By clicking "accept" in connection with completing this licensing transaction, you agree that the following terms and conditions apply to this transaction (along with the Billing and Payment terms and conditions established by Copyright Clearance Center, Inc. ("CCC"), at the time

that you opened your Rightslink account and that are available at any time at http://myaccount.copyright.com).

Limited License

With reference to your request to reprint in your thesis material on which Springer Science and Business Media control the copyright, permission is granted, free of charge, for the use indicated in your enquiry.

Licenses are for one-time use only with a maximum distribution equal to the number that you identified in the licensing process.

This License includes use in an electronic form, provided its password protected or on the university's intranet or repository, including UMI (according to the definition at the Sherpa website: http://www.sherpa.ac.uk/romeo/). For any other electronic use, please contact Springer at (permissions.dordrecht@springer.com or permissions.heidelberg@springer.com). The material can only be used for the purpose of defending your thesis limited to university-use only. If the thesis is going to be published, permission needs to be re-obtained (selecting "book/textbook" as the type of use).

Although Springer holds copyright to the material and is entitled to negotiate on rights, this license is only valid, subject to a courtesy information to the author (address is given with the article/chapter) and provided it concerns original material which does not carry references to other sources (if material in question appears with credit to another source, authorization from that source is required as well).

Permission free of charge on this occasion does not prejudice any rights we might have to charge for reproduction of our copyrighted material in the future.

Altering/Modifying Material: Not Permitted

You may not alter or modify the material in any manner. Abbreviations, additions, deletions and/or any other alterations shall be made only with prior written authorization of the author(s) and/or Springer Science + Business Media. (Please contact Springer at (permissions.dordrecht@springer.com or permissions.heidelberg@springer.com)

Reservation of Rights

Springer Science + Business Media reserves all rights not specifically granted in the combination of (i) the license details provided by you and accepted in the course of this licensing transaction, (ii) these terms and conditions and (iii) CCC's Billing and Payment terms and conditions.

Copyright Notice:Disclaimer

You must include the following copyright and permission notice in connection with any reproduction of the licensed material: "Springer and the original publisher /journal title, volume, year of publication, page, chapter/article title, name(s) of author(s), figure number(s), original copyright notice) is given to the publication in which the material was originally published, by adding; with kind permission from Springer Science and Business Media"

Warranties: None

Example 1: Springer Science + Business Media makes no representations or warranties with respect to the licensed material.

Example 2: Springer Science + Business Media makes no representations or warranties with respect to the licensed material and adopts on its own behalf the limitations and disclaimers established by CCC on its behalf in its Billing and Payment terms and conditions for this licensing transaction.

Indemnity

You hereby indemnify and agree to hold harmless Springer Science + Business Media and CCC, and their respective officers, directors, employees and agents, from and against any

and all claims arising out of your use of the licensed material other than as specifically authorized pursuant to this license.

No Transfer of License

This license is personal to you and may not be sublicensed, assigned, or transferred by you to any other person without Springer Science + Business Media's written permission.

No Amendment Except in Writing

This license may not be amended except in a writing signed by both parties (or, in the case of Springer Science + Business Media, by CCC on Springer Science + Business Media's behalf).

Objection to Contrary Terms

Springer Science + Business Media hereby objects to any terms contained in any purchase order, acknowledgment, check endorsement or other writing prepared by you, which terms are inconsistent with these terms and conditions or CCC's Billing and Payment terms and conditions. These terms and conditions, together with CCC's Billing and Payment terms and conditions (which are incorporated herein), comprise the entire agreement between you and Springer Science + Business Media (and CCC) concerning this licensing transaction. In the event of any conflict between your obligations established by these terms and conditions and those established by CCC's Billing and Payment terms and conditions, these terms and conditions shall control.

Jurisdiction

All disputes that may arise in connection with this present License, or the breach thereof, shall be settled exclusively by arbitration, to be held in The Netherlands, in accordance with Dutch law, and to be conducted under the Rules of the 'Netherlands Arbitrage Instituut' (Netherlands Institute of Arbitration).***OR:***

All disputes that may arise in connection with this present License, or the breach thereof, shall be settled exclusively by arbitration, to be held in the Federal Republic of Germany, in accordance with German law.

Other terms and conditions:

v1.3